

Modeling Study of a Proposed Vertical Evacuation Structure Site for the Shoalwater Bay Tribe

Final Project Report

February, 2020

L.M. Adams¹, F.I. González², R.J. LeVeque¹

¹University of Washington Applied Mathematics

²University of Washington Earth and Space Sciences

Study funded by the Federal Emergency Management Agency and the Shoalwater Bay Indian Tribe

Contents

| | |
|--|-----------|
| Abstract | 3 |
| 1.0 Introduction | 4 |
| 1.1 Background | 4 |
| 1.2 ASCE-compatible Sources and Scenarios | 4 |
| 1.3 Narrative of Maximum Considered Tsunami Scenario | 6 |
| 2.0 Development of ASCE-compatible CSZ Seismic Sources | 7 |
| 3.0 The MCT Scenario and Simulation Results | 9 |
| 3.1 MCT Impact on the VES Site. | 9 |
| 3.2 Warning, Tsunami Arrival and Evacuation Times | 12 |
| 4.0 Modeling Uncertainties and Limitations | 13 |
| 4.1 Tide stage | 13 |
| 4.2 Subsidence and uplift | 13 |
| 4.3 Structures | 13 |
| 4.4 Bottom friction | 13 |
| 4.5 Tsunami modification of bathymetry and topography | 13 |
| 5.0 Summary and Discussion | 14 |
| Acknowledgements. | 15 |
| References | 15 |
| Appendix A. ASCE 7 Compliance | 18 |
| A.1 Source Compliance with Offshore Tsunami Amplitude Criteria | 18 |
| A.2 Compliance with Sea Level Rise Criteria | 26 |
| A.3 Sea Level Rise, Subsidence, Uplift and Land Loss | 27 |
| A.4 Determination of MH, the Minimum Height of the Lowest Occupiable Level | 29 |
| A.5 Review and Approval of this Study | 32 |

Abstract

A Maximum Considered Tsunami (MCT) scenario was developed that includes projected sea level rise of 0.47 m over 75 years and a magnitude 9 tsunamigenic earthquake on the Cascadia Subduction Zone; development of the scenario is compliant with our current understanding of the 2016 American Society of Civil Engineers (ASCE) Building Code 7, i.e., ASCE 7-16, and was reviewed by a SEFT Peer Review Team and Peer Review Advisory Panel for the project. The results of the numerical simulation support the design of a vertical evacuation structure, a tower located within the city of Tokeland, WA on land purchased by the Shoalwater Bay Indian Tribe. Estimates of key hazard design parameters at the site include 75 years of sea level rise to 0.47 m above the current level, seismic subsidence of -2.5 m, maximum flooding of 5 m and maximum current speed of 6.7 m/s, all referenced to mean high water (*MHW*). The arrival times of the leading edge and the maximum amplitude of the first wave to arrive at the site are 29 and 36 minutes, respectively. Hazardous tsunami waves continue to arrive for the 6 hours of the simulation and would likely continue for as many more. Most of the peninsula will be flooded twice daily at mean high water to a depth of 1-3 m for decades, assuming that post-seismic uplift eventually raises the land above mean high water.

1.0 Introduction

The probability that an earthquake of magnitude 8 or greater will occur on the Cascadia Subduction Zone (CSZ) in the next 50 years has been estimated to be 10-14% (Petersen, et al., 2002). The last such event occurred in 1700 (Satake, et al., 2003; Atwater, et al., 2005) and future events are expected to generate a destructive tsunami that will inundate Shoalwater Bay Tribal land, the community of Tokeland, and many other Washington Pacific Coast communities within tens of minutes after the earthquake main shock. Project Safe Haven identified many of these communities and potential sites within each community for Vertical Evacuation Structures (Project Safe Haven Team, 2016).

1.1 Background

On 26 June 2018, the Shoalwater Bay Indian Tribe was awarded a Federal Emergency Management Agency (FEMA) Hazard Mitigation Assistance (HMA) grant for the design and construction of a Vertical Evacuation Structure (VES). Structural engineers responsible for the design of a VES require an assessment of the tsunami impact on the proposed site, including estimates of the maximum values of tsunami flooding, current speed and momentum flux that a VES must survive. The decision was made to design and construct a tsunami safe haven VES in the form of a tower at the site shown in Figure 1.

This report documents the methodology and results of a tsunami hazard assessment modeling study conducted for the site of the Shoalwater Bay VES Tower, in order to numerically model a geophysically credible and defensible "Maximum Considered Tsunami" (MCT) scenario to provide the information needed by structural engineers to design the VES tower; these results could also help guide community planning and mitigation of the impact on residents and infrastructure.



Figure 1. Left: Willapa Bay and Grays Harbor on the Washington Pacific Coast. **Right:** The Tokeland Peninsula; labeled symbols mark the locations of the Shoalwater Bay Casino, the VES site area (SwTwr & Gauge 403), the Tokeland community, and a sea level rise (SLR)

1.2 ASCE-compatible Sources and Scenarios

In what follows, we distinguish between *sources* and *scenarios*; *scenarios* are developed by numerical

simulation of tsunami generation by a *source* and the subsequent propagation and inundation of the VES site. More generally, however, *a new and distinct scenario is created by any modification of a model that produces a change in the corresponding simulation results*; examples include changes in topographic grids, friction parameters, reference sea level, etc.

Modeling studies of Vertical Evacuation Structure (VES) sites differ from community-level hazard assessment modeling studies in that design criteria for VES have been published by the American Society of Civil Engineers (ASCE)/Structural Engineering Institute (SEI), in the 2016 edition of the ASCE 7 Standard “Minimum Design Loads and Associated Criteria for Buildings and Other Structures” (ASCE, 2017). This publication is referred to as ASCE 7-16, and includes a new Chapter 6 “Tsunami Loads and Effects” as guidance for the design of tsunami vertical evacuation structures. This ASCE 7-16 standard is applicable to the states of Alaska, Washington, Oregon, California, and Hawaii, and has also been included in the requirements of the 2018 International Building Code (IBC18). In addition, the ASCE/SEI 7 Tsunami Loads and Effects Subcommittee (TLES) periodically reviews and votes on proposed revisions for the 2022 version of the ASCE 7 Standards in order to clarify criteria, resolve ambiguities and address issues that are encountered in the course of proposed VES site hazard assessment studies.

This study had the benefit of consultations and reviews of the work by a Peer Review Team (PRT) led by the SEFT (Structural Earthquake Forensic Tsunami) Consulting Group and a Peer Review Advisory Panel (PRAP), each of which included members of the ASCE TLES. This was fortunate, since the modeling and design criteria are relatively new and the TLES continues to clarify and improve this guidance.

Washington State has not formally adopted the ASCE 7-16 Chapter 6 standard for such studies ; nonetheless, this Shoalwater VES project has adopted these standards, as well as ASCE 7-22 Balloted Proposals that have been approved by a vote of the TLES, in anticipation of their acceptance by the ASCE 7 Main Committee and publication in 2022. However, since this ASCE guidance has only recently been developed and published, each application may uncover ambiguities or scientific/engineering issues that must be addressed in consultations with TLES members (Ian Robertson and Gary Chock) in order to move forward and complete the project. Those issues are documented in a separate report (Adams, et al., 2019b) which will be submitted to the TLES for review and resolution. Thus, notwithstanding such ASCE issues that have not been formally resolved, we have conducted informal discussions with ASCE 7-16 TLES members to obtain guidance on how to proceed and have conducted and completed this study with our best understanding of what is considered ASCE-compatible at this time and, most likely, in 2022; as such, we identify this study and its products and results as "ASCE-compatible."

ASCE 7-16 guidance is based on a probabilistic concept of a Maximum Considered Tsunami (MCT) characterized by a 2% probability of being exceeded in a 50-year period, or a 2,475-year mean recurrence interval (frequently rounded to a 2,500-year MCT in the literature). Chock (2016) states that “*The ASCE 7 Tsunami Loads and Effects chapter is consistent with the principles of probabilistic hazard analysis, tsunami physics, and fluid mechanics, integrated into a comprehensive set of design provisions.*” Thio (2010) describes an approach to developing probabilistic tsunami hazard maps for California; this approach was also used to develop the 2500-year MCT and an associated online ASCE Tsunami Design Geodatabase (TDG) Version 2016-1.0 (<https://asce7tsunami.online/>) on which ASCE 7-16 guidance is based.

Chapter 6 of ASCE 7-16 entitled "Tsunami Loads and Effects," authored by the ASCE 7 Tsunami

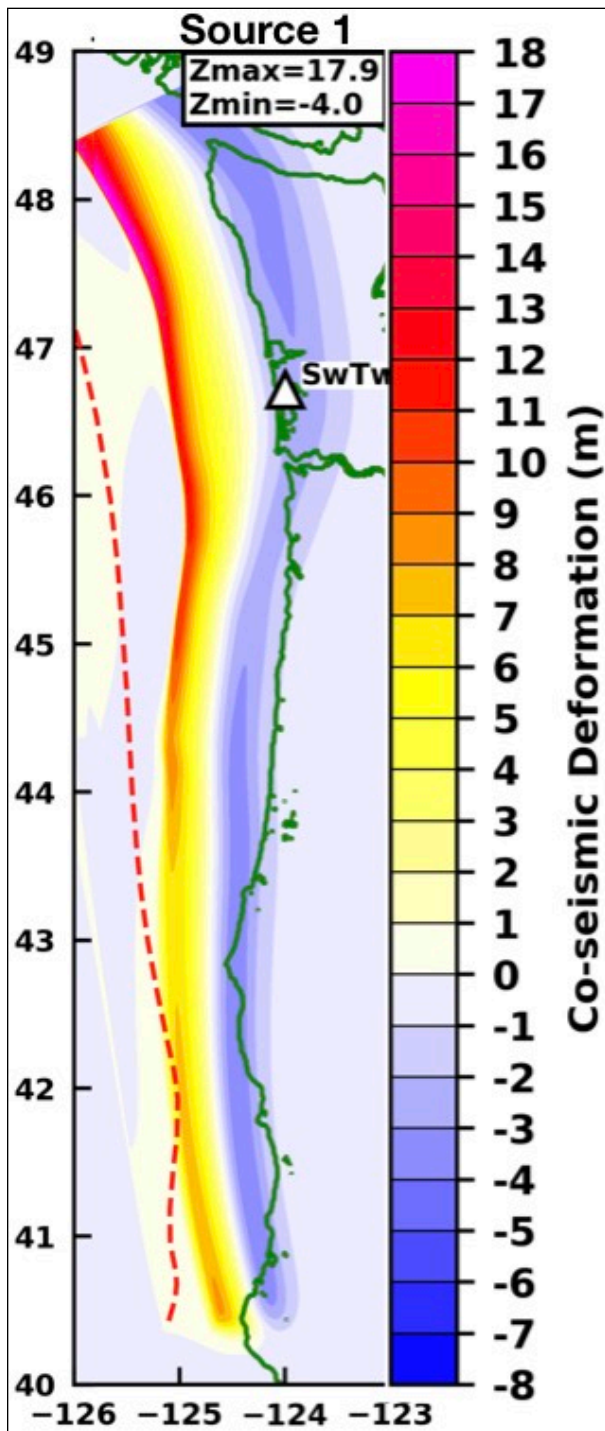


Figure 2. Deformation field of Source 1, which generates the Maximum Considered Tsunami (MCT). Warm colors are uplift, cool colors are subsidence, the white triangle marks the location of the VES site, and the dashed red line marks the trench and intersection of the Cascadia fault with the ocean floor.

Loads and Effects Subcommittee (TLES) provides criteria for development of the MCT. Section 2 defines the MCT as "A probabilistic tsunami having a 2% probability of being exceeded in a 50-year period or a 2,475-year mean recurrence interval" and Section 6.5.3 requires that "The direct physical effects of potential relative sea level change shall be considered in determining the maximum inundation depth during the project lifecycle. A project lifecycle of not less than 50 years shall be used." In addition, ASCE 7-16 provides criteria for the offshore tsunami amplitude (OTA) values that must be met to ensure ASCE-compatibility. Appendix A discusses these ASCE 7-16 compatibility criteria in more detail.

Figure 2 presents Source 1, which is based on a modified version of the Magnitude 9 seismic model, L1, developed by Witter et al. (2013) and, when used in a simulation that accounts for sea level rise (SLR), generates the Maximum Considered Tsunami (MCT) for this study. The development of this model is described in Appendix A. Note that the word "considered" in the MCT designation reflects the possibility that a more destructive or less destructive scenario could occur; this is because it is currently impossible to confidently forecast important details of the most fundamental aspects of the geophysical event we study in this report -- i.e., a great tsunamigenic earthquake on the CSZ. These important details include the time of occurrence (tomorrow ... in 20 years ... in 75 years ?), the magnitude of the earthquake (M8 ... M9 ... ?), and the severity and impact of the tsunami on individual communities at risk (maximum flooding ... maximum current speed ... ?). In the narrative presented next, we provide a brief description of the temporal evolution of the MCT and its impact on the VES site.

1.3 Narrative of Maximum Considered Tsunami Scenario

First, a cautionary note for the reader. The narrative that follows cannot be taken literally as an accurate, detailed prediction of what *will* happen; seismic and

tsunami models can provide valuable general guidance on what *may* happen, but large uncertainties exist in any seismic or tsunami model result. (This important reminder is also true for the rest of this document and Section 4.0 briefly describes a number of the most important uncertainties.) For this reason, qualifying terms such as "likely" and "may" are used liberally in this narrative. The narrative was developed for non-technical readers as a general but coherent story of how the impacts of a tsunamigenic earthquake on the residents and the physical environment of a community might evolve in time; it is based on collecting and organizing the results of our model simulations and other general, but well-known characteristics of great tsunamigenic earthquakes (such as the severity and duration of ground shaking) into a temporal framework.

The main shock of the M9 earthquake will likely be accompanied by strong shaking that will persist for 5 minutes or longer. There will be uplift offshore that generates a tsunami with a modeled maximum amplitude of about 12.5 m at a distance of about 80 km due west of the VES site (Figure 2 (b)) with the tidal stage at *MHW*. The VES site is currently about 1.5 m above *MHW*, but the seismic model indicates Willapa Bay will subside by about 2-3m and the subsidence at the VES tower site will be about 2.5 m, lowering the VES site to a level of 1.0 m *below MHW*; in addition, if the projected 75 year sea level rise (*SLR*) of about 0.47 m along the Shoalwater-Tokeland coastline has occurred (see Appendix A.2), then the level of the VES site below *MHW* will be about 1.5 m (Figures 4(a) and A5).

Model results indicate the first tsunami wave will arrive at the Shoalwater Bay Casino, the Shoalwater VES tower, and mid-town Tokeland in about 24, 29 and 34 minutes, respectively (Figure 4(b)), i.e., about 19, 24, and 29 minutes after approximately 5 minutes of severe shaking. The model also indicates the first wave will be the largest and as it propagates across the peninsula the maximum wave amplitude combined with the 2.5 m subsidence may produce maximum flooding at the VES site of about 5 m. Smaller amplitude but still dangerous waves continue to arrive periodically for the duration of the 6-hour simulation; although not modeled, dangerous waves are likely to continue for a number of additional hours before stopping entirely.

Post-tsunami, the seismic model indicates that at *MHW* the land in the VES tower area will be underwater by 1.5 m and at mean low water (*MLW*) it will be above water by 0.6 m. The *MHW* flood depth is due to subsidence of the base to a level 1.03 m below *MHW* plus a projected *SLR* of 0.47 m (Figures 4(a) and A5). The *MLW* exposure of the land is due to the mean tide range of 2.1 m at Toke Point, which is about 2 km distant from the VES; the mean tide range is defined as the difference of *MHW* and *MLW* (see <https://tidesandcurrents.noaa.gov/datums.html?id=9440910>). Assuming post-seismic uplift will occur, it may take decades to raise the peninsula above *MHW*.

2.0 Development of ASCE-compatible CSZ Seismic Sources

Guidance in ASCE 7-16 §6.7.2 recommends Cascadia, Alaska, and Kamchatka-Kuril seismic sources for a study site located in Washington. The [ASCE Tsunami Design Geodatabase](#) provides Disaggregated Hazard Source Contributions (DHSC) information in the form of figures such as Figure 3, for an Offshore Tsunami Amplitude (OTA) station at (-124.476, 46.68), directly offshore of the proposed Shoalwater VES Tower site. Not surprisingly, it is clear that Cascadia Subduction Zone (CSZ) seismic events dominate the contribution to OTA, compared to any far-field source regions. Consequently, we here ignore the far-field source regions and conduct this study using only near-field seismic events in CSZ; similarly, Wei, et al. (2017) also ignored far-field source regions in their study to produce the Tsunami Hazard Zones (THZ) included in the TDG.

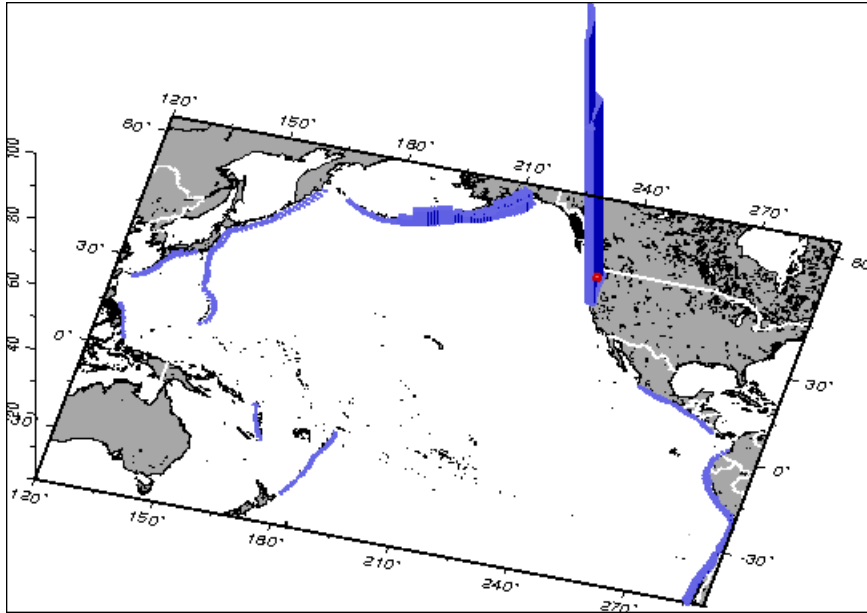


Figure 3. Disaggregated Hazard Source contributions for an offshore ASCE station at (-124.627, 46.969) directly west of the Aberdeen Stephens Elementary School VES study site, demonstrating the dominance of CSZ contributions to the OTA values.

For this modeling study of the VES site, the most important aspect of ASCE7-16 guidance is development of the tsunamigenic seismic source. This is because the fundamental tsunami parameters of most near-field tsunami modeling efforts are strongly dependent on spatial and temporal details of the source. In mathematical terms, the source specifies the initial conditions required to start the numerical computation of solutions to the governing partial differential equations in time and space and, generally speaking, different initial conditions produce different

solutions that describe tsunami generation, propagation and runup and, thus, the site-specific tsunami impact.

Also, with regards to sources other than a CSZ seismic event, ASCE 7-16, Section 6.7.2, states that other sources such as *"Local, nonsubduction zone seismic fault sources capable of moment magnitude of 7 or greater, including offshore and/or submarine fault sources that are tsunamigenic"* and *"Local coastal and submarine landslide sources documented in the recognized literature as being tsunamigenic of similar runup, as determined by historical evidence or having estimated probabilities within an order of magnitude of the principal seismic fault sources"* shall be considered *"to the extent that probabilistic hazards are documented in the recognized literature."* We are unaware of other types of sources that meet these criteria; consequently, only CSZ earthquake sources are considered in this study.

Witter et al. (2013) summarize the development of a suite of 15 seismic scenarios (5 magnitudes, each with 3 fault mechanisms) used in a study of Bandon, OR. Two of these scenarios, the "medium" size M1 and the "large" L1, are "splay fault" seismic models with estimated (magnitudes, recurrence periods) of (8.9 Mw, 1000 yrs) and (9.0 Mw, 3333 yrs), respectively. Because their maximum inundation lines encompass 80%–95% of the inundation lines of the other simulated tsunami inundation scenarios, Witter et al. (2013) suggest these as a credible alternative to consider for future revisions to coastal construction standards. Consequently, the peer-reviewed L1 scenario of Witter et al. (2013) has been used in a number of Washington State tsunami hazard assessment modeling studies (e.g., Gica and Arcas, 2016; Titov, et al., 23018; Adams, et al., 2019a). For this study, the L1 vertical deformation field is represented on a 10 arc-sec resolution rectangular grid as positive and negative values for uplift and subsidence, respectively. The grid was created by linear interpolation of an irregular grid of (longitude, latitude, vertical displacement) values

provided as a supplement to Witter, et al. (2011).

Modifications to the L1 deformation field were then made to develop a number of seismic sources that are compatible with ASCE guidance. In particular, an ASCE-compatible source generates a tsunami such that the modeled Offshore Tsunami Amplitude (OTA) meets the criteria found in ASCE 7-16 Chapter 6 and the Balloted Proposal §6.7.5.1/2 for inclusion in the 2022 revision, ASCE 7-22. Appendix A provides details of the development of these sources and the selection of Source 1 (Figure 2) as the basis for the MCT; see, in particular, Section A.1 and Table A1.

3.0 The MCT Scenario and Simulation Results

This study conducted all simulations with the GeoClaw model, which is part of Clawpack (Clawpack Development Team, 2017), and has undergone extensive verification and validation (e.g., Berger, et al., 2010; LeVeque, et al., 2011). GeoClaw has been accepted as a validated model by the US National Tsunami Hazard Mitigation Program (NTHMP) after conducting multiple benchmark tests as part of an NTHMP benchmarking workshop (González, et al., 2011). GeoClaw uses finite volume methods with adaptive mesh refinement and the finest grid resolution in and around the VES site was set to (longitude res, latitude res) = (1/3", 1/3") = (7.1 m, 10.3 m) at the latitude of the VES site.

3.1 MCT Impact on the VES Site.

Figure 4 presents results of the MCT simulation (based on Source 1 shown in Figure 2) in the form of contour maps of the maximum values (denoted by a caret) of $\hat{\zeta}$ (Greek zeta), \hat{s} and $\hat{\phi}$ (Greek phi) computed over the 6-hour simulation period, and the time series of h , s and ϕ recorded by Gauge 403 at the VES site (see Figures 1 and 2). Here h is the flow depth referenced to the topography, s is the current speed, $\phi = hss$ is the momentum flux, η is the wave amplitude referenced to MHW , and ζ is defined as h when onshore (pre-event) and as η when offshore (pre-event). As expected, this Scenario is associated with large values of \hat{h} , \hat{s} and $\hat{\phi}$. Furthermore, the combined effects of subsidence and SLR result in flooding of most of the peninsula at MHW with depths in the range of 2 - 8 m; a maximum flooding depth of 4.96 m was recorded by model gauge 403 at the VES site.

Table 1 summarizes key MCT simulation input parameters and output results and satisfies the primary goal of providing ASCE-compatible MCT parameters \hat{h} , \hat{s} and $\hat{\phi}$ at the VES site that are needed for the VES design process.

| Table 1. Maximum Considered Tsunami (MCT) Scenario key input and output parameters. B_0 , ΔB and B are the initial, co-seismic vertical displacement, and final values of the topography referenced to MHW , respectively. SLR is the sea level rise projected over 75 years. Gauge 403 recorded the Simulation Output at the VES site shown in Figure 1; see preceding text for parameter definitions. The minimum height (MH) and minimum build elevation (MBE), are quantities derived from the model output and are discussed in Appendix A. | | | | | | | | | | | | | | | | |
|---|--------------|-------|-------------------------|-----------|----------------|-----------|-------------------|---------------|-----------------|----------------------------|-----------------------------|---------|----------|-----------|-----------|------------|
| Scenario | Source Model | | Site Ground Deformation | | | SLR (m) | Simulation Output | | | | MH and MBE Computations | | | | | |
| | N | up | sb | B_0 (m) | ΔB (m) | | B (m) | \hat{h} (m) | \hat{s} (m/s) | $\hat{\phi}$ (m^3/s^2) | $\hat{\eta}$ (m) | S (m) | MH (m) | MH (ft) | MBE (m) | MBE (ft) |
| D | 1 | 1.172 | 1.000 | 1.46 | -2.49 | -1.03 | 0.47 | 4.96 | 6.70 | 206.65 | 3.93 | 3.05 | 9.19 | 30.14 | 10.65 | 34.93 |

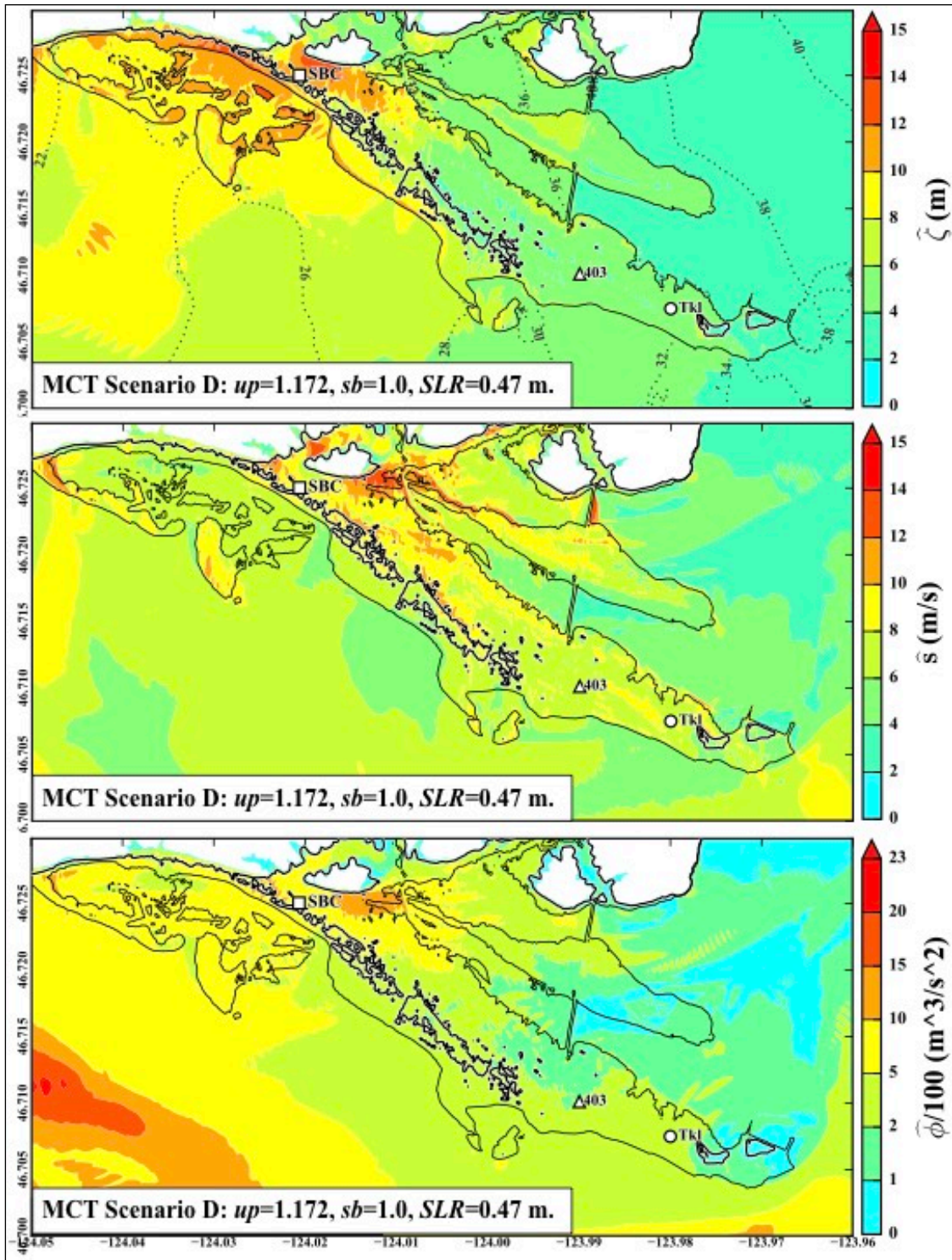


Figure 4(a). MCT Scenario D values of $\hat{\zeta}$, \hat{s} , $\hat{\phi}$ over 6-hrs, referenced to present-day MHW. Shoalwater Bay Casino, VES and model gauge 403, and Tokeland positions are white square, triangle and circle, respectively. Pre- and post-seismic coastlines are thin and thick black lines, respectively. Tsunami first arrival times (minutes) are light dotted lines in top plot of $\hat{\zeta}$.

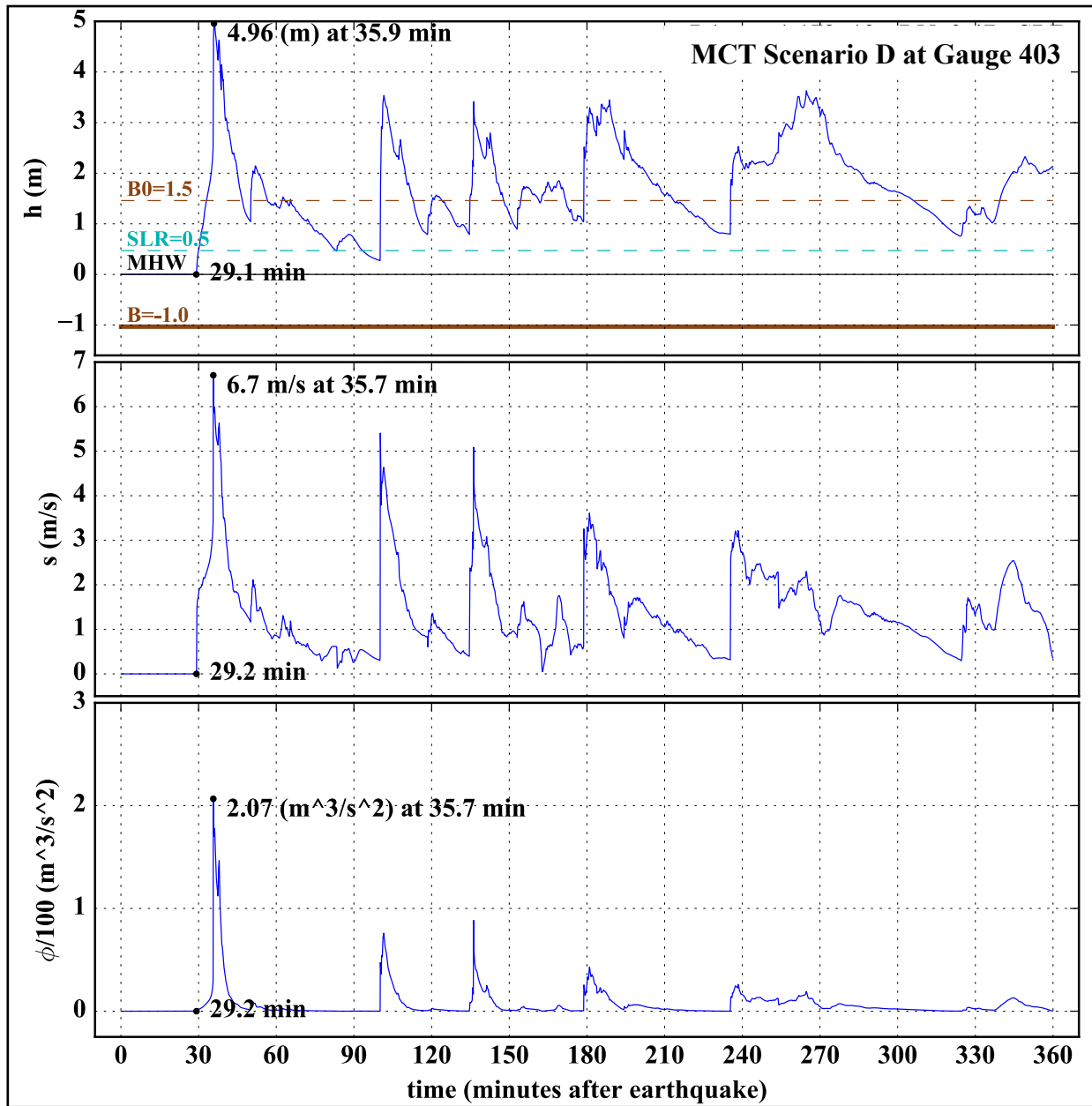


Figure 4(b). Modeled time series of h , s , ϕ at Gauge 403.

A total of 7 Scenarios were developed and Appendix A provides descriptions of different scenario characteristics and features, and a summary of key results for all 7 Scenarios in Table A1, from which Table 1, above, is extracted. All 7 sources in Table A1 are, in principal, ASCE-compatible. However an analysis focused primarily on geophysical credibility and defensibility narrowed candidates for the MCT source down to Source 1 (see Section A.1). We therefore adopted Source 1 for the MCT and included a projected 75-year SLR of 0.47 m (Miller, et al., 2018) in the simulation to comply with the ASCE 7 SLR criteria and create the ASCE-compatible MCT Scenario D.

Note that SLR was incorporated into the GeoClaw simulations of the MCT (and Scenario F) by

increasing the initial water level for the simulation above MHW by 0.47 m, the projected SLR over 75 years; but note that all elevations are still referenced to the present-day MHW, which is the vertical datum of the coastal topography DEM. Hence B_0 still refers to the present-day elevation of the topography and B to the post-quake elevation that incorporates subsidence, also relative to present-day MHW. Hence the values of B_0 and B in Table A1 are the same for the MCT as for the scenarios without SLR, and Figure 4 contours are of the present-day B_0 , not the future coastline after *SLR*. Also note that the change in tidal dynamics due to the associated increase in water depth is small, and so we assume that MHW rises by the same amount (0.47 m) as MSL rises. This is justified by modeling experiments conducted by Pickering, et al. (2017), in which changes in MHW on the US West Coast were estimated to agree with changes in MSL to within 1% even for much greater changes in MSL (see their Figure 2).

3.2 Warning, Tsunami Arrival and Evacuation Times

Tsunami arrival times are also extremely important, as they provide estimates of the time available for evacuation to the VES refuge. Figure 4(a) indicates that the leading edge of the tsunami wave will arrive at a northwest point of the Tokeland Peninsula coast about 22 minutes after the earthquake main shock, then sweep southeast along the pre-seismic southern coastline (thin black line) and reach the southeast extent of the peninsula in about 38 minutes. At the VES site itself, Figure 4(b) indicates the leading edge and first maximum of the wave will arrive about 29.1 and 35.9 minutes after the main shock, respectively; however, note that the onset of life-threatening conditions, i.e. flooding depth and current speed (h,s) increase to (1 m, 2 m/s) within minutes of the leading edge arrival; the implication of this is that residents on the peninsula must reach the VES refuge within about 30 minutes after the main shock.

The evacuation time, i.e., the actual length of time available for duration, is 30 minutes minus the warning time or, if longer than the warning time, the duration of shaking strong enough to prevent evacuation. It is most likely that strong shaking will provide the early warning and evacuation can begin once the severity of the shaking decreases to an allowable level; note that strong shaking during a subduction zone megaquake can persist for several minutes. It is unlikely that a so-called "tsunami earthquake" or "silent earthquake" will occur (Kanamori, 1972), in which the severity of coastal shaking can be too low to alarm; but if the earthquake is tsunamigenic, then it is large enough to be detected instrumentally, and a warning will be issued. In this case, then, evacuation would be delayed by the effectiveness of an earthquake and tsunami early warning (ETEW) system to deliver the warning to individual residents (LeVeque, et al., 2018).

4.0 Modeling Uncertainties and Limitations

GeoClaw uses the shallow water equations to model the tsunami, which is an approximation of the three-dimensional fluid dynamics, but one that has been found to be sufficiently accurate for inundation studies of this nature in previous studies, including validation and benchmarking workshops. However, it is only an approximation to the correct physics. A number of other assumptions or approximations are also made, as summarized below.

4.1 Tide stage

The simulations were conducted with the background sea level set to *MHW* for all Scenarios listed in Table A1 and set to *MHW + SLR* for Scenarios D and F. The *MHW* value is conservative, in the sense that the severity of inundation will generally increase with a higher background sea level. Larger tide levels do occasionally occur, but the assumption of *MHW* is standard practice in studies of this type.

4.2 Subsidence and uplift

This ground motion is taken into account in both source models used, and it is the underwater vertical motion that generates the tsunami. For both events, the details of the motion depend on the hypothetical earthquake source used, and this is the biggest source of uncertainty in the model results since the next earthquake may be very different from the ones that have been modeled.

4.3 Structures

Buildings were not included in the simulations, the topographic DEMs provided for this study are “bare earth”. The presence of structures will alter tsunami flow patterns and generally impede inland flow. To some extent the lack of structures in the model is therefore a conservative feature, in that their inclusion would generally reduce inland penetration of the tsunami wave. However, as in the case of the friction coefficient, impeding the flow can also result in deeper flow in some areas. It can also lead to higher fluid velocities, particularly in regions where the flow is channelized, such as when flowing up streets that are bounded by buildings.

4.4 Bottom friction

Mannings coefficient of friction was set to 0.025 in GeoClaw, a standard value used in tsunami modeling that corresponds to gravelly earth. This value is conservative in some sense, because the presence of trees, structures and vegetation would justify the use of a larger value, which might tend to reduce the inland flow. On the other hand, larger friction values can lead to deeper flow in some areas, since the water may pile up more as it advances more slowly across the topography.

4.5 Tsunami modification of bathymetry and topography

Severe scouring and deposition are known to occur during a tsunami, undermining structures and altering the flow pattern of the tsunami itself. Again, this movement of material requires an expenditure of tsunami energy that tends to reduce the inland extent of inundation. On the other hand, if natural berms or ridges along the coastline (or man-made levies or dikes) are eroded by the tsunami, then some areas can experience much more extensive flooding. There is no erosion or deposition included in the simulations presented here.

5.0 Summary and Discussion

A tsunami hazard assessment modeling study was conducted to support the structural engineering design of a VES tower to be located in Tokeland, WA, on property owned by the Shoalwater Bay Indian Tribe. An ASCE-compatible "Maximum Considered Tsunami" scenario was developed, simulated, and designated as Scenario D. The numerical simulation provided output that included key hazard design parameters: 75 years of sea level rise by 0.47 m and seismic subsidence of -2.5 m, maximum flooding of 5 m and maximum current speed of 6.7 m. These results are summarized in Table A1.

Also of interest from the Emergency Management perspective are the arrival times at the site of the leading edge of the first wave and the arrival time of the maximum of the first wave, producing maximum flooding at the site at 29 and 36 minutes after the earthquake main shock, respectively (Figure 4(b)). Similarly, the duration of the hazard is of note; hazardous high waves continued to impact the site throughout the 6-hour duration of the simulation (Figure 4(b)) and might very well continue for many additional hours before the episodes of flooding and associated strong currents cease completely. Edge waves propagating along the continental shelf can impact the site many hours after the first tsunami wave. It is also possible that seiching in Willapa Bay may be triggered by the tsunami and/or sufficiently violent seismic deformation that might occur in the first few minutes of the event.

Note that the ASCE 7 guidance continues to evolve and improve. Adams, et al. (2019b) discusses some issues we encountered in the course of this study with ASCE 7 criteria. For example, the *SLR* projection data of Miller et. al (2018) is provided as probability of exceedance and would more properly be incorporated into the initial probabilistic methodology.

Acknowledgements.

This project was jointly funded by FEMA and the Shoalwater Bay Indian Tribe and was performed in consultation with Cale Ash and Hee Jae Yang of Degenkolb Engineers. Ian Robertson and Gary Chock provided very helpful feedback and suggestions on our study. Discussions with Yong Wei were also very helpful, and he kindly provided the parameters of the seismic source developed by Wei et. al. (2017) designated in this study as Source 2.

References

- Adams, L., F. Gonzalez, and R. LeVeque (2019a), Tsunami Hazard Assessment of Whatcom County, Washington, Project Report – Version 2, http://staff.washington.edu/rjl/pubs/THA_Whatcom .
- Adams, L.M., F.I. González, R.J. LeVeque (2019b): Issues in the Development of ASCE-Compatible Seismic Sources, University of Washington ResearchWorks Archive: <http://hdl.handle.net/1773/43827>.
- ASCE (2017): Minimum design loads and associated criteria for buildings and other structures. ASCE/SEI 7-16. Reston, VA: ASCE.
- Atwater, B.F., and E. Hemphill-Haley (1997): Recurrence intervals for great earthquakes of the past 3,500 years at northeastern Willapa Bay, Washington: U.S. Geological Survey Professional Paper 1576, 108 p., <https://pubs.er.usgs.gov/publication/pp1576>.
- Atwater, Brian F., Musumi-Rokkaku Satoko, Kenji Satake, Tsuji Yoshinobu, Ueda Kazue, and David K Yamaguchi (2005): USGS Professional Paper 1707, pp 1–144.
- Berger, M. J., D. L. George, R. J. LeVeque, and K. T. Mandli (2010): The GeoClaw software for depth-averaged flows with adaptive refinement. Preprint and simulations: www.clawpack.org/links/papers/awr10 .
- Chock, Gary Y. K. (2016): Design for Tsunami Loads and Effects in the ASCE 7-16 Standard, J. Struct. Eng., 2016, 142(11): 04016093.
- Clawpack Development Team, Clawpack software, 2017, <https://doi.org/10.5281/zenodo.820730>, <http://www.clawpack.org>. Version 5.4.1.
- Gica, E. and D. Arcas(2016): Tsunami Inundation Modeling of Anacortes and Bellingham, Washington due to a Cascadia Subduction Zone Earthquake. PMEL Tech report, ftp://newportftp.pmel.noaa.gov/tsunami/WaEMD/Anacortes_Bellingham/documentation/Anacortes_Bellingham_Washington_Report.pdf.
- González, F., R. J. LeVeque, J. Varkovitzky, P. Chamberlain, B. Hirai, and D. L. George, (2011): GeoClaw Results for the NTHMP Tsunami Benchmark Problems, <http://depts.washington.edu/clawpack/links/nthmp-benchmarks/geoclaw-results.pdf> .
- Hemphill-Haley, E., (1995): Diatom evidence for earthquake-induced subsidence and tsunami 300 yr ago in southern coastal Washington: Geological Society of America Bulletin, v. 107, no. 3, p. 367-378.

- Kanamori, H., (1972): Mechanism of tsunami earthquakes, *Physics of the Earth and Planetary Interiors*, 6, 346-359.
- Kemp, Andrew C., Niamh Cahill, Simon E. Engelhart, Andrea D. Hawkes, Kelin Wang, (2018): Revising estimates of spatially variable subsidence during the A.D. 1700 Cascadia earthquake using a Bayesian foraminiferal transfer function, *Bulletin of the Seismological Society of America* 108 (2): 654-673. <https://doi.org/10.1785/0120170269>)
- Leonard, L. J., R. D. Hyndman and S. Mazzotti (2004). "Coseismic subsidence in the 1700 great Cascadia earthquake: Coastal estimates versus elastic dislocation models." *Geological Society of America Bulletin*, **116**(5).
- Leonard, Lucinda J., Claire A. Currie, Stéphane Mazzotti, Roy D. Hyndman (2010): Rupture area and displacement of past Cascadia great earthquakes from coastal coseismic subsidence, *GSA Bulletin*, 122 (11-12): 2079-2096. <https://doi.org/10.1130/B30108.1>
- LeVeque, R. J., D. L. George, and M. J. Berger, (2011): Tsunami modeling with adaptively refined finite volume methods, *Acta Numerica*, pp. 211–289.
- LeVeque, R.J., P. Bodin, G. Cram, B.W. Crowell, F.I. Gonzalez, M. Harrington, D. Manalang, D. Melgar, D.A. Schmidt, J.E. Vidale, C.J. Vogl, and W.S.D. Wilcock, (2018): Developing a Warning System for Inbound Tsunamis from the Cascadia Subduction Zone, Oceans 2018 conference, <http://hdl.handle.net/1773/43181> .
- Miller, I.M., Morgan, H., Mauger, G., Newton, T., Weldon, R., Schmidt, D., Welch, M., Grossman, E. (2018): Projected Sea Level Rise for Washington State – A 2018 Assessment. A collaboration of Washington Sea Grant, University of Washington Climate Impacts Group, Oregon State University, University of Washington, and US Geological Survey. Prepared for the Washington Coastal Resilience Project. <http://www.wacoastalnetwork.com/wcrp-documents.html>
- Petersen, M. D., C. H. Cramer, and A. D. Frankel (2002): Simulations of Seismic Hazard for the Pacific Northwest of the United States from Earthquakes Associated with the Cascadia Subduction Zone. *Pure Appl. Geophys.*, 159, 2147-2168. <https://doi.org/10.1007/s00024-002-8728-5>.
- Pickering, M.D., K.J. Horsburgh, J.R. Blundell, J.J.-M. Hirschi, R.J. Nicholls, M. Verlaane, N.C. Wells (2017): The impact of future sea-level rise on the global tides, *Continental Shelf Research* 142, 50–68.
- Project Safe Haven Team (2016): Project Safe Haven: Tsunami Vertical Evacuation on the Washington Coast, 42 pp, <https://mil.wa.gov/uploads/pdf/emergency-management/final-report-2016-11-21-16.pdf>
- Satake, Kenji, Kelin Wang and Brian F Atwater (2003): Fault Slip and Seismic Moment of the 1700 Cascadia Earthquake Inferred From Japanese Tsunami Descriptions, *Journal of Geophysical Research* 108 (B11): 1–17. doi:10.1029/2003JB002521.

- Shennan, I., A. J. Long, M. M. Rutherford, F. M. Green, J. B. Innes, J. M. Lloyd, Y. Zong and K. J. Walker, (1996): Tidal Marsh Stratigraphy, Sea-Level Change and Large Earthquakes, I: A 5000 Year Record in Washington, U.S.A., *Quaternary Science Reviews*, Vol. 15, pp. 1023-1059.
- Thio, H. K., Somerville, P. G., and Polet, J. (2010). "Probabilistic tsunami hazard in California." Pacific Earthquake Engineering Research Center Report. 108, 331, Berkeley, CA.
- Titov, V., D. Arcas, C. Moore, R. LeVeque, L. Adams, and F. Gonzalez, Tsunami Hazard Assessment of Bainbridge Island, Washington, Project Report, 2018, http://staff.washington.edu/rjl/pubs/THA_Bainbridge.
- Wang, P.-L., S. E. Engelhart, K. Wang, A. D. Hawkes, B. P. Horton, A. R. Nelson, and R. C. Witter (2013): Heterogeneous rupture in the great Cascadia earthquake of 1700 inferred from coastal subsidence estimates, *J. Geophys. Res. Solid Earth*, 118, 2460–2473, doi:10.1002/jgrb.50101.
- Wei, Y., H. Thio, V. Titov, G. Chock, H. Zhou, L. Tang, and C. Moore (2017): Inundation Modeling to Create 2,500-Year Return Period Tsunami Design Zone Maps for the ASCE 7-16 Standard, 16th World Conference on Earthquake Engineering, 16WCEE 2017, Santiago Chile, January 9th to 13th, 2017, Paper No. 450, 10 pp.
- Witter, R. C., et al. (2013). "Simulated tsunami inundation for a range of Cascadia megathrust earthquake scenarios at Bandon, Oregon, USA." *Geosphere* 9(6): 1783-1803.
- Witter, R. C., Y. Zhang, K. Wang, G. R. Priest, C. Goldfinger, L. L. Stimely, J. T. English, and P. A. Ferro (2011): Special Paper 43, Simulating tsunami inundation at Bandon, Coos County, Oregon, using hypothetical Cascadia and Alaska earthquake scenarios, 57 p. with supplement, including plates, GIS and data files, and animations (<https://www.oregongeology.org/pubs/sp/p-SP-43.htm>).

Appendix A. ASCE 7 Compliance

A.1 Source Compliance with Offshore Tsunami Amplitude Criteria

The ASCE criteria for offshore tsunami amplitude (OTA) are as follows:

OTA Criteria 1. *The extent of offshore tsunami amplitude points considered for the site include points within at least 60 km but not exceeding 80 km of projected length along the coastline, centered within a tolerance of plus or minus 10 km on the site*

OTA Criteria 2. *The values of computed OTA shall be not less than 80% of the coinciding OTA values given by the ASCE TDG.*

OTA Criteria 3. *The mean value of the computed OTA shall be at least 100% of the mean value for the coinciding OTA data provided in the ASCE TDG.*

Figure A1 presents the physical setting in which conformance with these criteria was developed, i.e., the locations of the OTA data provided in the online ASCE TDG relative to the VES site location. Also shown is the Miller, et al. (2018) SLR station closest to the VES site; the data for this site were used to satisfy the additional ASCE SLR criteria, as discussed in Section A.2, below.

Table A1 summarizes key input and output parameters associated with sources and scenarios developed in this study and the values of minimum *height (MH)* and minimum built *elevation (MBE)* of the lowest refuge level, which are discussed in Section A.4, below. Source 0 is the original, unmodified L1 model developed by Witter, et al. (2013) from which Sources 1, 3 and 4 were derived by multiplying the uplift and subsidence of the L1 deformation filed by the factors *up* and *sb*, respectively; Source 2 is the ASCE-compatible seismic model developed by Wei et al., (2017). A brief discussion of each source follows.

Source 0 is based on the original, unmodified L1 seismic model of Witter et al., (2013) for which the irregularly spaced deformation model data, $(x,y,\Delta B) = (\textit{longitude}, \textit{latitude}, \textit{vertical crustal deformation})$, was interpolated to a computational grid with 10 arc-second resolution.

Source 1 is a modification of Source 0 in which the uplift values were multiplied by the factor 1.172 to meet the ASCE criteria for Offshore Tsunami Amplitude and the original, unaltered subsidence values were retained to conform more closely to subsidence estimates at the site in peer-reviewed studies (see the discussion and justification for this approach, below).

Source 2 was developed on a 10 arc-sec grid using a linear combination of unit sources from the Short-term Inundation Forecasting for Tsunamis (SIFT) database (<https://nctr.pmel.noaa.gov/tsunami-forecast.html>). The seismic slip parameters were those determined by Wei, et al. (2017) to develop a source that is consistent with the ASCE guidelines for a portion of the Washington coast, for the purpose of developing maps of the Tsunami Design Zone (TDZ) that reside in the online ASCE Tsunami Design Geodatabase. Essentially, the TDZ maps define the maximum inland limits of flooding due to this source, and the purpose of the TDZ maps is described in the first paragraph of ASCE 7-16, Chapter 6, Section 6.1.1 Scope as *"The following buildings and other structures located within the Tsunami Design Zone shall be designed for the effects of Maximum Considered Tsunami, including hydrostatic and hydrodynamic forces, waterborne debris accumulation and impact loads, subsidence, and scour effects in accordance with this chapter: ... "* Thus, the question of whether or not a structure should be designed and constructed to be ASCE-compatible is governed by the TDZ maps, i.e., by whether or not the structure is inside the TDZ area.

Source 3 is a modification of Source 0 obtained by multiplying the uplift values by the factor $up=1.172$ to meet the ASCE criteria for Offshore Tsunami Amplitude and multiplying the subsidence values by the factor $sb=0.600$ to bring the modeled subsidence to within 3 cm of the value provided in the ASCE Tsunami Geodatabase.

Source 4 is a modification of Source 0 obtained by multiplying both the uplift and subsidence values by the factor $up=1.172$ needed to comply with the ASCE OTA criteria.

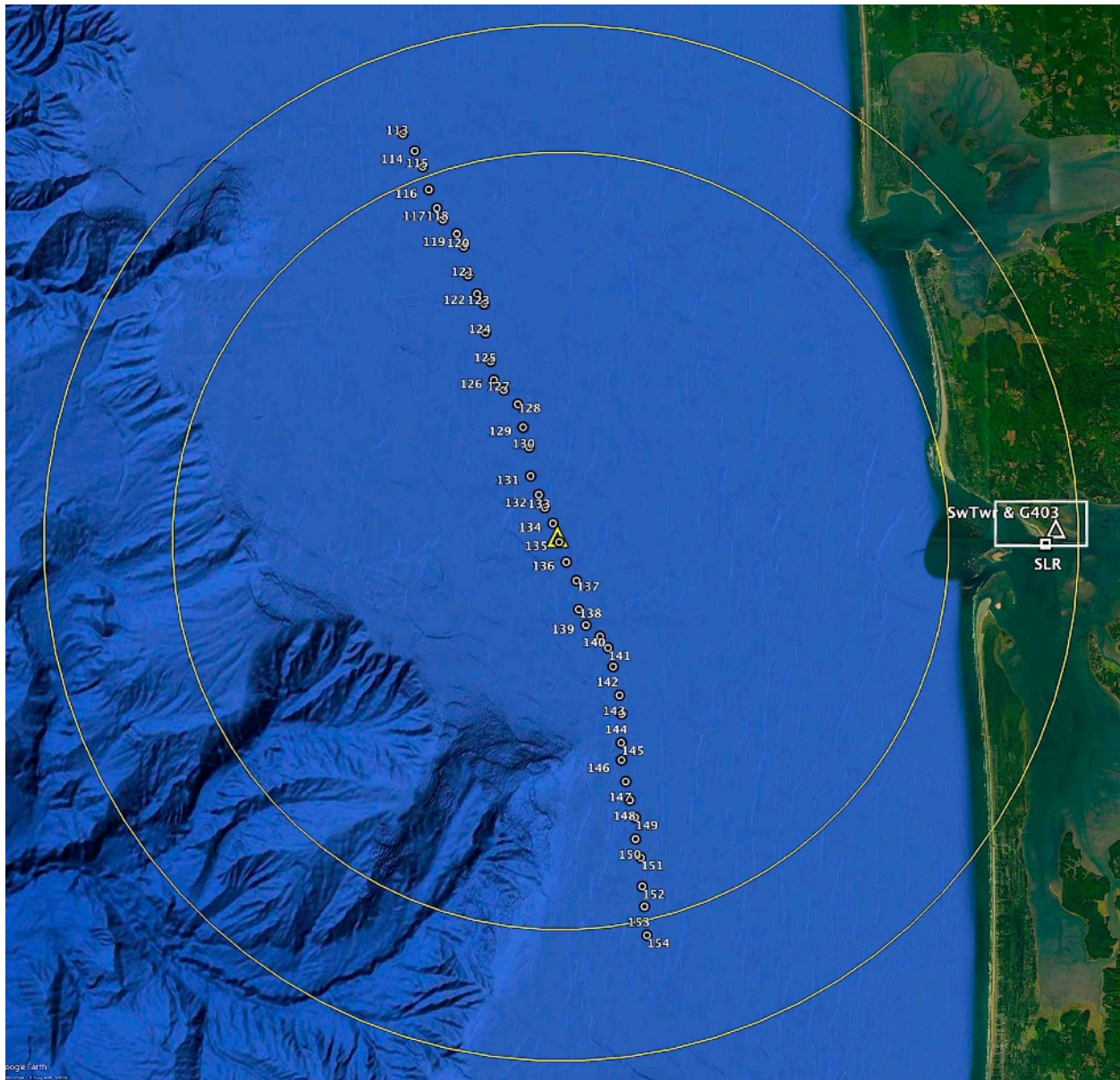


Figure A1. Location of the Shoalwater Tower site (white rectangle), the offshore ASCE OTA stations 113-154 (numbered circles) and the Miller, et al., 2018 SLR station closest to the VES site (white square). Yellow circles delineate radii of 30 and 40 km that encompass the OTA stations; center of circles (yellow triangle) is at the latitude of the VES, i.e., the white triangle labeled "SwTwr & G 403."

Table A1. Summary of Scenario input and output parameters, including the MCT for this study, Scenario D. All Scenarios used ASCE-compatible sources; however, only the MCT Scenario D and Scenario F are ASCE-compatible because they both account for *SLR*. All source models except Source 2 are based on the L1 seismic model in which uplift and subsidence values are multiplied by the factors *up* and *sb*, respectively; Scenario C uses Source 2, the model developed by Wei et al., (2017). Simulation output was recorded by gauge 403 at the VES site shown in Figure 1. The parameters B_0 , ΔB and B are the initial, co-seismic vertical displacement, and final values of the topography referenced to *MHW*, respectively. *SLR* is the sea level rise projected over 75 years. The next 4 columns provide maximum values (denoted by a caret over the parameter symbols) recorded during the entire 6-hour simulation -- they are: \hat{h} , the flow depth referenced to the local topography; \hat{s} , the current speed; $\hat{\phi}$, the momentum flux, and $\hat{\eta}$ the wave amplitude referenced to *MHW*. The minimum height (*MH*) and minimum build elevation (*MBE*), are quantities derived from the model output and are discussed in Section A.4, below.

| Scenario | Source Model | | | Site Ground Deformation | | | SLR (m) | Simulation Output | | | | MH and MBE Computations | | | | |
|----------|--------------|-----------|-----------|-------------------------|----------------|---------|---------|-------------------|-----------------|----------------------------|------------------|-------------------------|---------------|----------------|----------------|-----------------|
| | N | <i>up</i> | <i>sb</i> | B_0 (m) | ΔB (m) | B (m) | | \hat{h} (m) | \hat{s} (m/s) | $\hat{\phi}$ (m^3/s^2) | $\hat{\eta}$ (m) | S (m) | <i>MH</i> (m) | <i>MH</i> (ft) | <i>MBE</i> (m) | <i>MBE</i> (ft) |
| A | 0 | 1.000 | 1.000 | 1.46 | -2.49 | -1.03 | 0.00 | 3.93 | 5.84 | 128.28 | 2.90 | 3.05 | 7.85 | 25.75 | 9.31 | 30.54 |
| B | 1 | 1.172 | 1.000 | 1.46 | -2.49 | -1.03 | 0.00 | 4.56 | 6.57 | 177.56 | 3.53 | 3.05 | 8.67 | 28.44 | 10.13 | 33.23 |
| C | 2 | na | na | 1.46 | -0.96 | 0.50 | 0.00 | 3.47 | 4.55 | 69.13 | 3.96 | 3.05 | 7.70 | 25.25 | 9.16 | 30.04 |
| D | 1 | 1.172 | 1.000 | 1.46 | -2.49 | -1.03 | 0.47 | 4.96 | 6.70 | 206.65 | 3.93 | 3.05 | 9.19 | 30.14 | 10.65 | 34.93 |
| E | 3 | 1.172 | 0.600 | 1.46 | -1.49 | -0.04 | 0.00 | 4.34 | 6.90 | 179.08 | 4.31 | 3.05 | 8.69 | 28.50 | 10.15 | 33.28 |
| F | 3 | 1.172 | 0.600 | 1.46 | -1.49 | -0.04 | 0.47 | 4.69 | 6.77 | 192.39 | 4.65 | 3.05 | 9.13 | 29.95 | 10.59 | 34.73 |
| G | 4 | 1.172 | 1.172 | 1.46 | -2.92 | -1.46 | 0.00 | 4.72 | 6.25 | 169.94 | 3.26 | 3.05 | 8.75 | 28.70 | 10.21 | 33.48 |

Figure A2 compares OTA values for Sources 1 and 2 against the ASCE OTA data, demonstrating that that OTA Criteria 2 and 3 are satisfied by each source. For this ASCE OTA criteria test, the GeoClaw model resolution was set to 6 arc-seconds, i.e., (longitude, latitude) = (6", 6") = approximately (127 m, 185 m). Not shown in the figure are Sources 3 and 4, which are also rendered ASCE compatible by the same factor, *up*=1.172 even though they are associated with different subsidence factors, *sb*; their OTA values at each OTA station differ from the Source 1 values by no more than 11 cm and 5 cm, respectively.

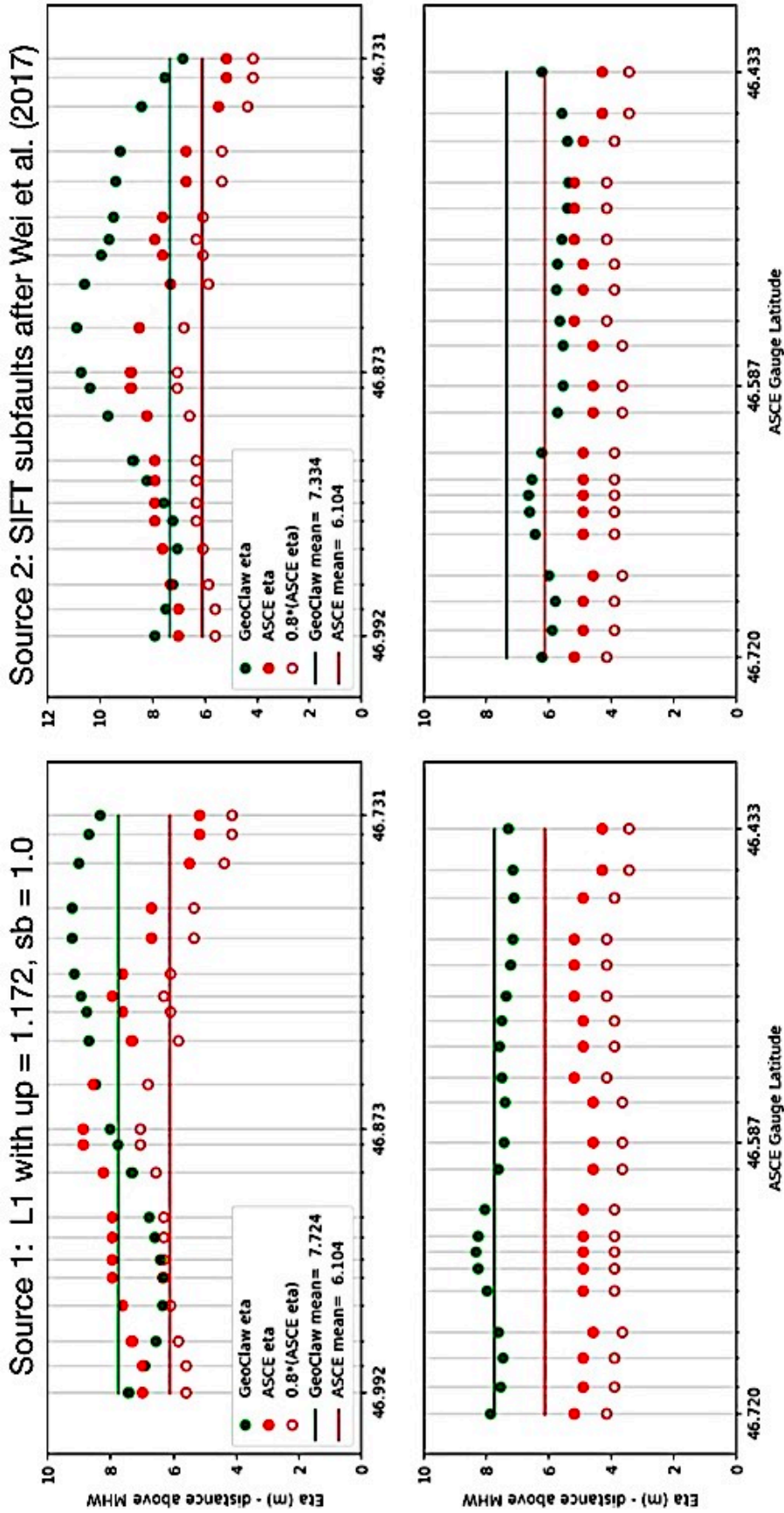


Figure A2. ASCE-compatibility plots demonstrating Sources 1 and 2. compliance with ASCE OTA criteria.

Although Sources 1 and 2 are both ASCE-compatible, they are quite different; this can be seen in the deformation patterns for the two Sources presented in Figure A3 for comparison. As discussed in Adams, et al. (2019b), there are multiple extrema in the deformation field of Source 2 that may be artifacts of slip discontinuities and mismatches at sub-fault edges.

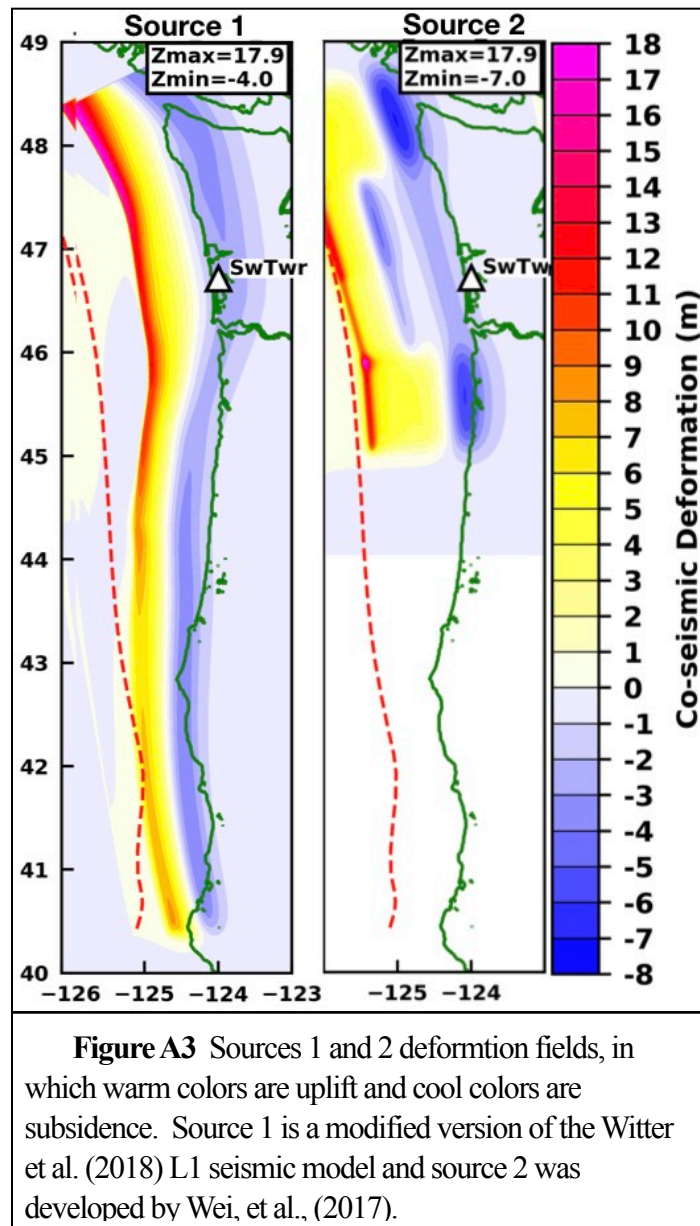


Figure A3 Sources 1 and 2 deformation fields, in which warm colors are uplift and cool colors are subsidence. Source 1 is a modified version of the Witter et al. (2018) L1 seismic model and source 2 was developed by Wei, et al., (2017).

Moreover, the slip of Source 2 was placed primarily on the subfaults farther offshore (closer to the trench), which resulted in the associated subsidence being shifted farther off-shore relative to Source 1; Source 2 also caused considerably less subsidence at the VES site than Source 1 (Table A1). As a consequence of these differences, the potential impact on the Washington coast and on the Shoalwater VES site is less severe.

Therefore, because Source 1 has a greater impact on the VES site than Source 2, and because Washington State has used the L1 source in a number of tsunami hazard assessment studies, we did not use Source 2 to develop an ASCE-compatible MCT scenario. Rather, as indicated in Table A1, Source 1 was used to develop Scenario D, the ASCE-compatible MCT Scenario, by including the effects of *SLR* (see Section A.2).

However, two features of Sources 1, 3 and 4 raise concerns. First, the OTA of all three appear to be overly conservative. Second, Source 4 subsidence of -2.92 m at the VES site also appears extreme in the context of recent peer-reviewed literature on the topic of Cascadia coseismic coastal deformation; in fact, this concern is what led to the consideration of Sources 1 and 3. These two concerns are discussed next.

Concern 1. Overly Conservative OTA of Sources 1, 3 and 4. The OTA mean value of these Sources, for which the factor $up=1.172$ are about 25% greater than the ASCE OTA mean value (Figure A2). (Similarly, the OTA mean value of source Source 2 is about 20% greater than the ASCE OTA mean value.) It was suggested that L1 slip values be adjusted to provide a better fit of the GeoClaw and ASCE OTA. Although ASCE 7-16 does not currently provide quantitative criteria regarding the fit of model OTA to ASCE OTA, several requests were made to obtain the L1 slip values but we have not received those files, to date. During review of the project by the PRT, PRAP and other stakeholders, consensus was reached by all that the conservatism was acceptable and the project was able to move forward (see Section A.5).

Concern 2. Overly Conservative Subsidence at the VES site. The ASCE TDG provides a value of -1.4 m subsidence at the VES site and recent literature on Cascadia subsidence suggests an upper limit for coastal subsidence due to Cascadia megaquakes to be about -2 m. However, Sources 1 and 4 produce values of -2.49 m and -2.92, respectively (Table A1). Since the degree of subsidence at the site is a critical factor in the severity of the tsunami impact, we here investigate which of Sources 1, 3 or 4 is most appropriate, given that each uses a different value of the subduction factor, sb .

Note that any value other than $sb = up$ is geophysically questionable, because it implies that the processes of uplift and subsidence during a seismic event are independent. However, noting that there is also significant and inherent uncertainty in seismic source specification, we believe that if the difference in tsunami impact on the VES site is small when sources with $sb = up$ and $sb \neq up$ are compared, and if this value $sb \neq up$ improves agreement of VES subsidence with the peer-reviewed literature on Cascadia coastal subsidence, then the use of $sb \neq up$ is justified.

Source 4 is obtained by multiplying the entire L1 deformation field by the factor $sb=1.172$, so that the value of -2.49 m at the VES site is increased to -2.92 m (Table A1). Early studies suggest that maximum subsidence values of up to 3 m might be within the range of field data accuracy. However, more recent studies that were conducted with more and/or better subsidence estimates suggest that this upper limit of 3 m is too large and that the upper subsidence limit is more likely in the range of 1-2 m. Wang et al. (2013) provide a history of paleoseismic estimates of Cascadia coseismic coastal subsidence in their Section 2.1. A brief summary of a few of these studies follows.

Early studies include Hemphill (1995), who used fossil diatoms from four stratigraphic sections along the tidal Niawiakum River, southwestern Washington, to provide an independent paleoecological test of a relative sea-level rise and found the paleoecological changes observed at these sites could have ranged from a minimum of 0.8 – 1.0 m to a maximum of about 3.0 m during the Cascadia 1700 event (see the Abstract of that report); Atwater and Hemphill-Haley (1997) extended this work to more sites in the general locality, characterizing their findings with the less quantitative phrase "subsidence of at least 1 m" (see page 83 of their report). Similarly, the Shennan, et al. (1996) field study, which used ecological interpretations of microscopic fossils to describe eight inferred earthquakes over the past 5,000 years in Grays Harbor reported "probably about 1.5 m" subsidence with a possible range of 1.45 m to 3.1 m at a station in the Johns River (see page 1095 of their report).

More recently, however, four studies all suggest that maximum coastal subsidence is more likely in the 1 - 2 m range. The 1700 Cascadia event study by Leonard, et al. (2004) used elastic dislocation models constrained by interseismic geodetic and thermal data and a compilation of available estimates of coastal coseismic subsidence from previous paleoelevation studies (see their Figure 6). The 1700 Cascadia event study by Wang, et al. (2013) applied transfer function analyses to field data to produce improved subsidence estimates to constrain dislocation models and developed a "preferred" model that featured heterogeneous slip (see their Figure 6). The 1700 Cascadia event study by Kemp, et al. (2018) focused on developing, testing and applying four increasingly sophisticated transfer functions to the existing field data to further improve the subsidence estimates and compare them with the preferred dislocation model of Wang, et al. (2013) (see their Figures 5 and 10). Finally, in contrast to these 3 studies of the single 1700 Cascadia event, Leonard, et al. (2010), examined 9 Cascadia events over 6,500 years; dislocation models of these past megathrust events were constrained by a compilation of coseismic vertical displacement estimates at coastal

marsh sites based on soil horizons, radiocarbon data, event correlations with megathrust-triggered turbidites, and estimates of megathrust slip based on comparisons of marsh displacements. This study reached several conclusions that bear on the issue of event-to-event variability and are therefore particularly relevant to this and other site-specific tsunami hazard assessment studies, as follows.

1. *"Comparison between events shows that mean subsidence values are 0.1–0.6 m in coastal southern British Columbia (Vancouver Island; A.D. 1700 event only), 1.0–1.6 m in southern Washington, 0.4–0.9 m in northern Oregon, 0.7–1.2 m in southern Oregon, and 0.7–0.95 m in northern California."*
2. *"Most of the full- or nearly full-margin earthquakes recorded in the sediments, including the most recent great earthquake in A.D. 1700, exhibit subsidence similar to these values. Exceptions include events T2 and 5a, which showed little to no displacement in southern Washington and northern Oregon, and the A.D. 1700 earthquake, which had higher than average subsidence in that region."*
3. *"The consistency of subsidence values among events presently detectable within the data limitations indicates that there is limited variability in rupture behavior between earthquakes, and that hazard analyses based on an average Cascadia event and its uncertainties provide a useful predictor of the subsidence and slip expected in future megathrust earthquakes."*

Comparing maximum flooding values at the VES site for Scenarios B, E and G in Table A1, we see that for $sb = (1.172, 1.0, 0.60)$ we have $\hat{h} = (4.72, 4.56, 4.34)$ m, respectively, so that the reductions, $d\hat{h} = (0.16$ m, 0.22 m), are relatively small; furthermore changes in the physical impact of each source on the site as judged by the momentum flux, are also relatively small $\hat{\phi} = (169.94, 177.56, 179.08)$ (m^3/s^2) and $d\hat{\phi} = (7.62, 1.52)$ (m^3/s^2), or less than 1%. Also, by examining time series at the VES site in Figure A4, we see that the temporal evolution of the series for sb factors 1.172 and 1.000 display only small differences, while differences in the time series for $sb = 0.600$ are more easily discernible.

Based on these results the source with the 1.0 subsidence factor, Source 1 was chosen as the MCT for this study. This approach serves to reduce extreme subsidence values somewhat with minimal changes to the tsunami impact on the VES site. Subsequently, although the independent adjustments of uplift and subsidence imply an independence of the uplift and subsidence processes that is geophysically questionable, the PRAP and PRT noted that it did not violate ASCE 7-16 criteria as currently written and found this approach acceptable (see section A.5).

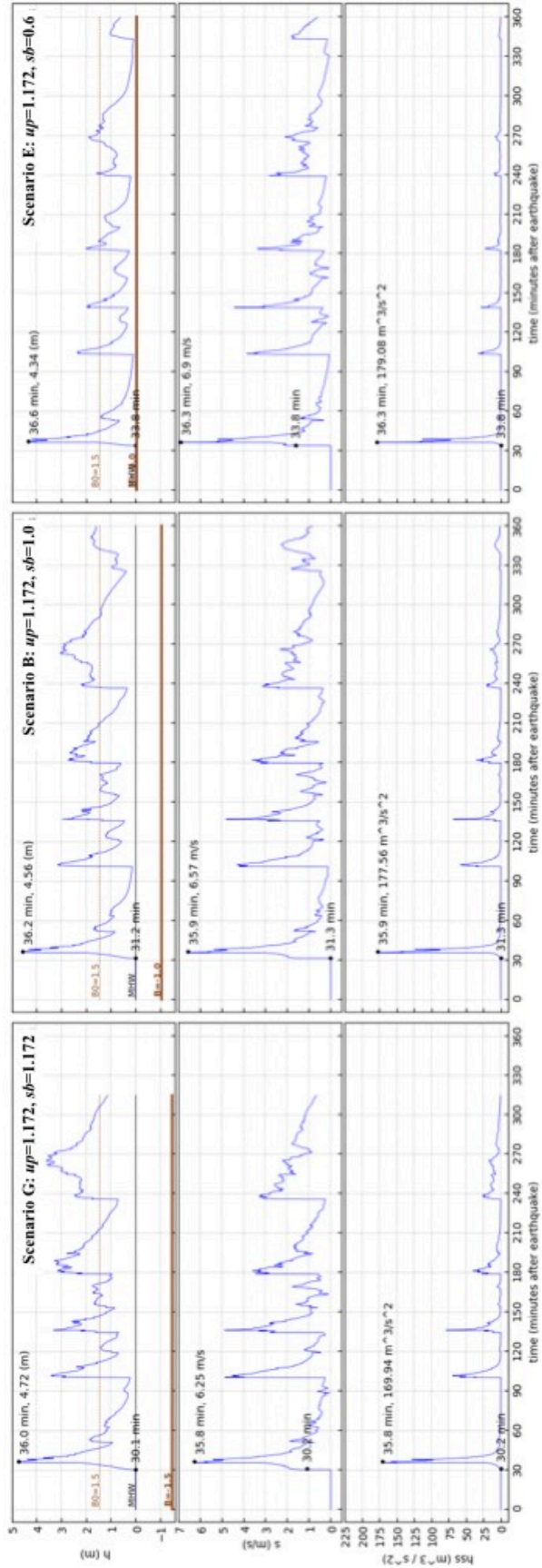


Figure A4. Gauge 403 time series at the VES site of flooding depth, speed and momentum for Scenarios G, B and E modified by the factors up and sb listed in Table A1.

A.2 Compliance with Sea Level Rise Criteria

Although Source 1 conforms to the ASCE OTA criteria and is therefore ASCE-compatible, a *Scenario* must also account for projected *SLR* over the project lifecycle in order to be ASCE compatible. ASCE 7-16 Section 6.5.3 states that *"The direct physical effects of potential relative sea level change shall be considered in determining the maximum inundation depth during the project lifecycle. A project lifecycle of not less than 50 years shall be used."* The project lifecycle for this project was chosen to be the design life of the VES, i.e., 75 years. Assuming construction is completed in 2020, the *SLR* projection corresponds to the year 2095.

The projections of Miller, et al. (2018) are summarized in a series of excel files that can be downloaded at <http://www.wacoastalnetwork.com/wcrp-documents.html> . They were produced for each of 171 coastal locations on a 0.1-degree grid for two greenhouse gas Representative Concentration Pathway (RCP) scenarios corresponding to low and high levels of emissions designated as RCP 4.5 and RCP 8.5, respectively.

The Excel file corresponding to the high greenhouse gas emission scenario RCP 8.5 for the coastal station closest to the VES site (at 46.7N, 124.0W) was used to create Table A2, below. The original projections are given as *SLR* values in feet that are associated with probabilities that range from 0.1% - 99% that a value will be exceeded by a given year ranging from 2010 - 2050, in decadal increments. Feet were converted to meters and values for 2045 and 2095 were obtained by linear interpolation. The range of probabilities in Table A2 were those identified in the study as members of the "likely" category. For the ASCE-compatible Scenario D, this hazard assessment study of the Shoalwater VES site chose to use the intermediate "Central Estimate" of 50% as the probability that *SLR* will exceed 0.47 m over the next 75 years.

For compatibility with ASCE 7, Section C6.5.3 suggests the historic sea level trend presented by <https://tidesandcurrents.noaa.gov/sltrends/sltrends.html> be used for a minimum 50 year life cycle. The Toke Point trend is given as 0.43 mm/year with a confidence interval of +/- 0.85 mm/year, for a maximum trend of 1.28 mm/year that results in a 75-year projection of 96 mm, much less than the 470 mm projection used here.

Table A2. Projected Sea Level Rise (m) at the location shown in Figure A1. Columns are the Center Year of a 19-year assessment period and the probability that the projected *SLR* will be exceeded before the Center Year. The table is based on Miller, et al. (2018), in which probability of exceedance values of 17% - 83% are identified as the "likely range" and the value of 50% is known as the "Central Estimate."

| Center Year | 83% | 50% Central Estimate | 17% |
|-------------|------|----------------------|------|
| 2045 | 0.08 | 0.12 | 0.18 |
| 2070 | 0.15 | 0.27 | 0.40 |
| 2095 | 0.27 | 0.47 | 0.67 |

A.3 Sea Level Rise, Subsidence, Uplift and Land Loss

Coastal uplift (or, less likely, subsidence) can occur between earthquakes, as part of the "earthquake deformation cycle" and can be an important component of the apparent changes in background sea level changes. Typically, a subduction zone earthquake creates sudden coastal land subsidence, which is then followed by decades or centuries of slow coastal land uplift. Miller et al. (2018) take this interseismic land deformation into account and thus formally designate their estimates as "Relative Sea Level Change." ASCE 7 guidance uses both this formal term in, for example, definitions, but Sea Level Rise in discussion of criteria. Since only sea level rise occurs in the region of interest, we adopt the term Sea Level Rise (*SLR*).

Figure A5 presents the effects of subsidence in the 3 scenarios and, in the case of the MCT Scenario D, the additional effect of projected *SLR* over 75 years. The significant difference between Scenarios B and C in the amount of land submerged at *MHW* is apparent. In Scenario B, almost the entire peninsula is submerged at *MHW*, in contrast to the much smaller coastal land area submerged in Scenario C. The peninsula is relatively flat, so that the 1.5 m difference between Scenarios B and C, i.e., -2.5 m and -1 m, makes a large difference in the degree of *MHW* flooding.

The MCT Scenario D flooding is, of course, even more extensive when the effect of a 0.47 m rise in sea level is added, as shown in Figure A5. Post-tsunami, then (as described in the Narrative, Section 1.3) the seismic model indicates that at *MHW* the land in the VES tower area will be underwater by 1.5 m and at mean low water (*MLW*) it will be above water by about 0.6 m. The *MHW* flood depth is due to subsidence of the base to a level 1.03 m below *MHW* plus a projected *SLR* of 0.47 m (Figures 4(a) and A5). The *MLW* exposure of the land is due to the mean tide range of 2.1 m at Toke Point, which is about 2 km distant from the VES; the mean tide range is defined as the difference of *MHW* and *MLW* (see <https://tidesandcurrents.noaa.gov/datums.html?id=9440910>). Assuming post-seismic uplift will occur, it may take decades to raise the peninsula above *MHW*.

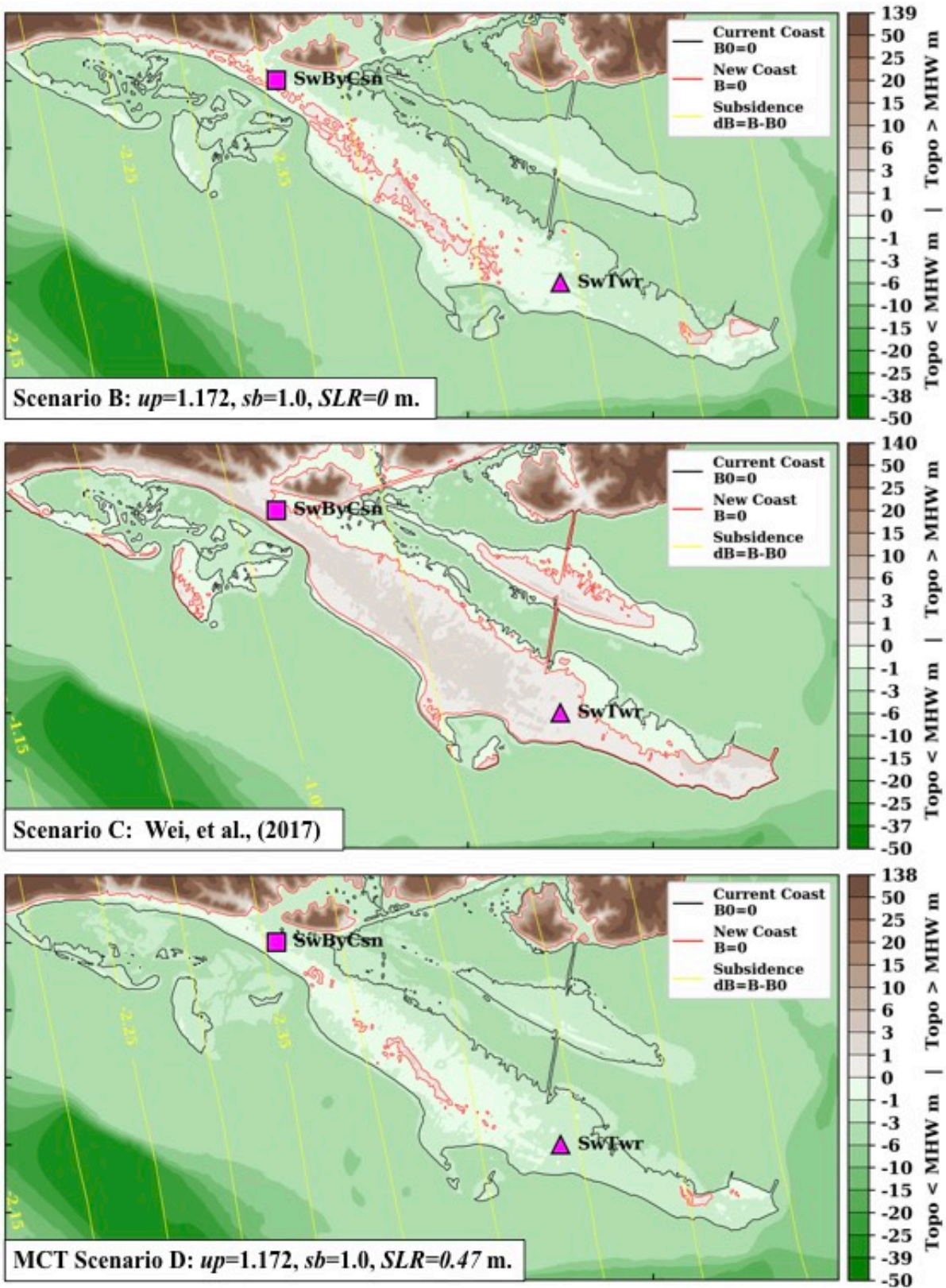


Figure A5. Land loss due to the effects of local subsidence and, in the case of the Maximum Considered Tsunami, Scenario D, the additional effect of projected *SLR* over 75 years.

A.4 Determination of *MH*, the Minimum Height of the Lowest Occupiable Level

It is essential to have a value for the minimum *height* of the lowest refuge level (*MH*) before construction as part of the required input to the design of the structure. ASCE 7-16 does not provide such an expression explicitly, but it can be derived from the definition of the minimum *elevation* (*ME*) of the lowest refuge level defined in Section 6.14.1 "*Minimum Inundation Elevation and Depth*" of ASCE 7-16, which states that

"Tsunami refuge floors shall be located not less than the greater of 10 ft (3.05 m) or one-story height above 1.3 times the Maximum Considered Tsunami inundation elevation at the site as determined by a site-specific inundation analysis, as indicated in Fig. 6.14-1."

Thus *ME*, the minimum *elevation* of the lowest refuge level, is defined as

$$ME = 1.3 \hat{\eta} + S \quad (1)$$

where the overhead caret symbol is adopted to denote maximum values of parameters, so that $\hat{\eta}$ is the maximum inundation *elevation* referenced to *MHW*, and $S = \max(10 \text{ feet}, 1 \text{ story})$ is a safety factor.

Note that a distinction is made between *elevation* and *height* or *depth* levels throughout Chapter 6 of ASCE 7-16; levels referenced to *MHW* are designated *elevations* and levels referenced to the grade plane (*GP*) are designated *heights* or *depths*. Thus, the required *MH* is referenced to the *GP* and, for pre-construction design purposes, we need an expression of *MH* as a function of the site-specific modeling results. (Since the exact grade plane elevation, *GP*, is unknown before construction, we assume in what follows that *GP* is coincident with the existing local topography and we caution that any changes to the existing local topography that creates a non-coincident *GP* must be taken into account when computing the *MH*.)

The physical setting for (1) is illustrated in Figure A6, which reproduces a revised version of Figure 6.14.-1 provided in the ASCE 7 Change Proposal Form, *File TS-CH06-04r00, Relating to revising the reference datum from NAVD88 to Mean High Water (MHW)*. This document was submitted to the ASCE 7 Main Committee on 9/13/2018 to propose the following revision to ASCE 7-16

*INUNDATION ELEVATION: The elevation of the design tsunami water surface, including relative sea level change, with respect to vertical datum at ~~in~~ *North American Vertical Datum (NAVD-88 Mean High Water (MHW)*.*

in which strike-throughs denote the existing ASCE 7-16 text and underlines denote the proposed changes to be published in the revised 2022 version, i.e., ASCE 7-22. Note that the above definition of *inundation elevation* requires that *relative sea level change* must be taken into account. In this study, the change is due to sea level rise, *SLR*. Therefore, with regards to equation (1), it is important to note that

- (a) it accounts for both co-seismic deformation and *SLR* because the numerical simulation of all scenarios is conducted with the co-seismic deformation inherent in the earthquake source and the initial water level adjusted by *SLR*, and
- (b) it applies specifically to the Post-Event situation, i.e., after the tsunami has flooded the site to the maximum depth, \hat{h} , and after any alteration of the VES site topography has occurred by co-seismic

deformation, and that

- (c) if co-seismic deformation does move the structure vertically with respect to the constant reference level, MHW in this study, then the Pre-Event value of ME will differ from the Post-Event value by the local deformation, ΔB (as determined in the discussion that follows).

Figure A7 schematically illustrates the Pre- and Post-Event situation at the VES site and we first examine the Post-Event panel on the right, in which we see that the minimum *elevation* of the lowest refuge level (ME) has been constructed according to the definition given by (1) and that the minimum height, MH , is given by

$$MH = ME - B$$

To obtain MH as a function of the site-specific inundation modeling output, we insert equation (1) for ME to obtain

$$MH = 1.3 \hat{\eta} + S - B \quad (2)$$

as the minimum *height* of the lowest occupiable refuge level, MH , in an expression that allows computation and use in the design process before construction. It is important to note in Figure A7 that the maximum depth of the water is $\hat{\eta}$ minus the post-quake elevation of the site, B , and that when computing this depth (and the required height of the first occupiable level of the VES), one must use the post-quake (subsided) site elevation B , not the initial pre-quake elevation, B_0 .

Turning to the Pre-Event panel we see that, once the structure has been built, the minimum *build elevation* of the lowest refuge level, here designated MBE , will be

$$MBE = MH + B_0$$

and by inserting (2) for MH and using $B = B_0 + \Delta B$, we obtain MBE in terms of the site-specific modeling results as

$$MBE = 1.3 \hat{\eta} + S - \Delta B$$

or, using (1)

$$MBE = ME - \Delta B$$

which, as mentioned above, identifies the difference between Pre- and Post-Event ME values as the local deformation value, ΔB . In the case of subsidence, $\Delta B < 0$ and so $MBE > ME$; with this in mind, we can see this graphically by comparing the Pre- and Post-Event panels in Figure A7.

Table A1 provides MH and MBE for the Scenarios developed during this study and described in Section A.1. As indicated in Table A1, the MBE value for Scenario D, the MCT for this study, is 10.65 meters or 34.93 feet. Also note the small range of MBE values for all Scenarios of 1.49 meters or 4.89 feet, suggesting a moderate insensitivity of the equation for MBE , above, to modest changes in the input parameters ΔB (-2.49 m to -0.96m) and SLR (0 m to 0.47 m).

Note also that the additional water level at the site represented by the quantity ($SLR - \Delta B$) of 0.96 m in Scenario C and 2.96 m in MCT Scenario D, a difference of 2 m, produces MBE values that are closer, 9.16 m and 10.65 m, respectively, or a difference of 1.49 m. In spite of this, MCT Scenario D has an impact on

the VES site that is 3 times greater than Scenario C, as indicated by the values of maximum momentum flux, $\hat{\phi}$, of 206.65 (m^3/s^2) and 69.13 (m^3/s^2), respectively.

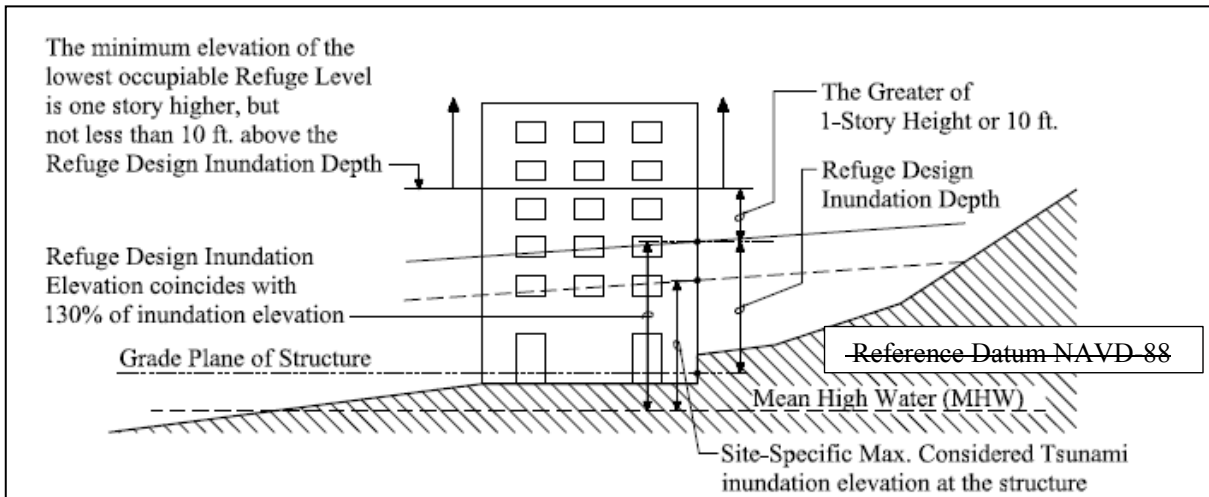


FIGURE 6.14-1 Minimum Refuge Level Elevation [1 ft = 0.305 m]

Figure A6. Reproduction of Figure 6.14-1 as presented in ASCE 7 Change Proposal Form, identified as *File TS-CH06-04r00, Relating to revising the reference datum from NAVD88 to Mean High Water (MHW)*. Strike-throughs denote the existing ASCE 7-16 text and underlines denote proposed changes to the existing text to be published in the revised 2022 version, i.e., ASCE 7-22

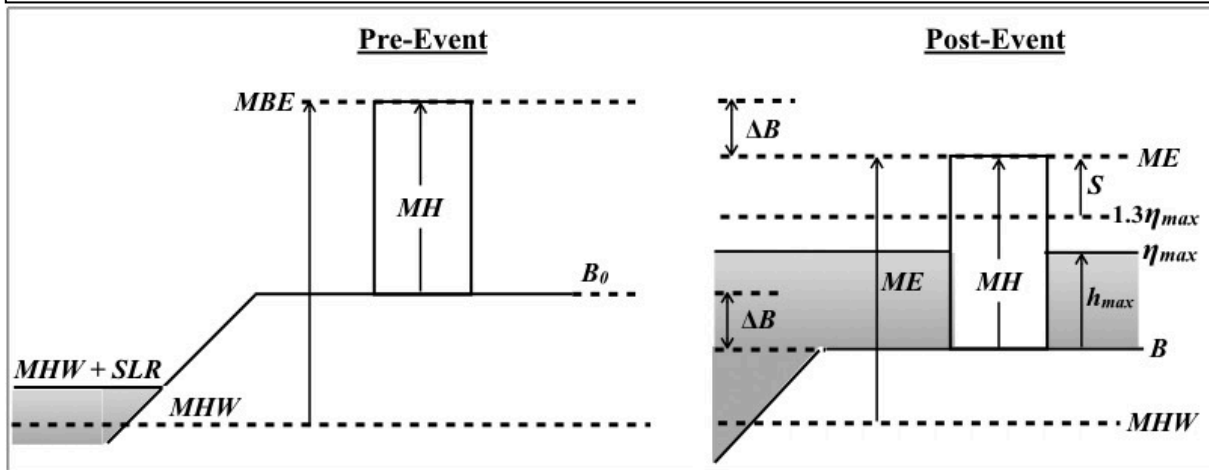


Figure A7. Left: Pre-Event geometry, showing VES minimum height to the lowest refuge level, MH , referenced to local topography, B_0 . (Local grade plane level, GP , is assumed accounted for by B_0 .) Before performing the tsunami simulation, water level is adjusted to include SLR . **Right:** Post-Event geometry with co-seismic subsidence $\Delta B < 0$. Here $B = B_0 + \Delta B$ is the subsided elevation, and $\hat{\eta}$ is the maximum tsunami inundation elevation at this location. **Note:** Inundation elevation η is related to the inundation depth, h , by $\eta = h + B$ and the values B_0 , B , η , ME , and MBE are all elevations relative to the unchanging vertical datum MHW , while MH and h are respectively a height and water depth referenced to the local topography. This figure is for the case when $\Delta B < 0$ and the subsided topography is still above MHW , but the formulas hold in other cases as well, including $\Delta B \geq 0$.

A.5 Review and Approval of this Study

As mentioned in Section 1.2, this study had the benefit of consultations and reviews of the work by a Project Advisory Panel (PAP) and a Peer Review Team (PRT) led by the SEFT (Structural Earthquake Forensic Tsunami) Consulting Group, each of which included members of the ASCE TLES. After distribution of a draft of this report, a teleconference was held on 10 September 2019 with representatives of PAP, PRT, Degenkolb Engineers, the Shoalwater Bay Indian Tribe (SBIT) and our UW Modeling Team. A consensus was reached that this study be approved and the results accepted as input to the design and construction of the VES site. The draft minutes of that teleconference are reproduced below, in Figure A8. Subsequently, minor revisions were made to the report and it was submitted for final approval. The email confirming acceptance of the final report by the Project Advisory Panel, the Peer Review Team, Degenkolb Engineers, and the Shoalwater Bay Indian Tribe is reproduced below, in Figure A9.



**Shoalwater Bay Indian Tribe Tsunami Evacuation Tower Peer Review:
Tsunami Inundation Modeling Discussion**

Date: September 10, 2019
Time: 9:30 AM to 11:00 AM (PDT)

Attendees:

Owner/Owner’s Rep

Shoalwater Bay Indian Tribe -Lee Shipman
OAC Services (Owner’s PM) -Mitchell Romero

Design Team

Degenkolb (Prime) -Cale Ash
University of Washington -Frank Gonzalez, Loyce Adams, Randy LeVeque

Peer Review Advisory Panel

ATC/University of Hawaii -Ian Robertson
University of Washington -Bob Freitag
WA DNR -Corina Forson, Daniel Eungad, Tim Walsh
WA EMD -Maximilian Dixon, Tim Cook

SEFT Peer Review Team

SEFT -Kent Yu, Jim Newell
AECOM -Hong-Kie Thio

General Meeting Description:

The primary purpose of this meeting was to discuss tsunami modeling peer review comments with the design team and owner and reach consensus on a modeling approach that will result in a successful project (i.e., safe, on time, and within budget).

Specific Discussion Items:

1. ASCE 7-16 Compliance – Discussed that goal was to reach consensus on a modeling approach that integrated compliance with the ASCE 7-16 national standard and local practice in the State of Washington (L1 scenario). Ian discussed that according to ASCE 7-16 the computed offshore tsunami amplitude values must on average match or exceed the ASCE Tsunami Design Geodatabase and that no individual points should be less than 80% of the geodatabase. For this project the L1 scenario has been increased by approximately 17% to meet this 80% minimum requirement. When looking at the onshore inundation depths, the L1 scenario (without the 17% increase) is more conservative than the ASCE geodatabase. This may be due to the fact that the ASCE digital elevation model (DEM) is based on a 60-90 meter grid spacing, where the site

Signed: Kent Yu and Jim Newell – SEFT



specific study DEM is based on a 10 meter grid spacing, or other factors. Even with the L1 scenario inundation depth being greater than the ASCE geodatabase inundation depth, the offshore matching requirement remains and the L1 scenario needs to be increased by approximately 17% to satisfy this ASCE requirement.

2. Sea-level Rise – Discussed that sea-level rise needs to be appropriately considered for the projected design life of the structure (75 years). Refuge elevation is relatively insensitive to sea-level rise and the 0.47 meter value being used by the design team is more conservative than ASCE 7 requirements.
3. Path Forward – All parties were in agreement that using the currently proposed modeling approach (17% increase on L1 scenario, including sea-level rise) satisfies ASCE 7 requirements and will result in a safe design for the evacuation tower.
4. Cost Impact – Degenkolb indicated that a cost estimate is in the process of being developed based on the design team’s Design Development (DD) documents. The design presented in those drawings is based on some potentially conservative design assumptions for geotechnical and tsunami modeling (inundation depth and flow velocity) that has been progressing concurrently with the structural design. The team felt that project construction cost would be relatively insensitive to a minor change in the elevation of the tsunami refuge level. Discussed that if the cost estimate exceeds the project budget, it might be necessary to revisit the tsunami modeling to reduce potential conservatism.
5. Energy Grade Line Analysis – Corina raised a question related to a conflicting statement in the Basis of Design document about Energy Grade Line (EGL) Analysis. Cale indicated that EGL analysis to check the minimum flow velocity had not been conducted due to a lack of the overtopped inundation depth data for the Tokeland Peninsula. Ian indicated that this data is available, and Cale indicated that Degenkolb will perform the EGL check on minimum flow velocity.

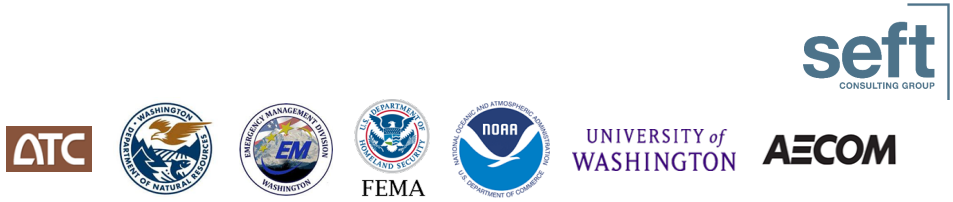
Action Required: Provide Degenkolb with overtopped inundation depth data for Tokeland Peninsula (originally provided by Ian).

By: Kent Yu, SEFT

6. Bigger Picture – Discussed that this project has brought to light questions about the modeling approach and appropriate implementation of the tsunami modeling provisions of ASCE 7-16. These are bigger picture questions that are not possible to be resolved in the context of the current SBIT project. Ian took note of the discussion and will bring the desire for additional clarity in the development of probabilistic offshore wave heights back to the ASCE 7 Tsunami Load and Effects Subcommittee. He also invited interested parties to apply for membership in the ASCE 7 Tsunami Loads and Effects Subcommittee to help in refinement of the provisions. Corina indicated that there is a group within the National Tsunami Hazard Mitigation Program that will likely be engaging in discussions with the ASCE subcommittee soon.

Signed: Kent Yu and Jim Newell – SEFT

Page 2 of 3



7. Closing Remarks – Lee and Mitch thanked the team for their diligence and passion in working with SBIT to deliver a successful project.

DRAFT

Signed: Kent Yu and Jim Newell – SEFT

Page 3 of 3

Figure A8. Draft minutes of 10 September 2019 teleconference between representatives of PAP, PRT, Degenkolb Engineers, the Shoalwater Bay Indian Tribe and the UW Modeling Team.



Frank I. Gonzalez <figonzal@uw.edu>

RE: Shoalwater Bay Tsunami Evacuation Tower Peer Review Comment Log

1 message

Kent Yu <kentyu@seifconsulting.com>
Thu, Feb 6, 2020 at 9:06 AM
To: "Frank I. Gonzalez" <figonzal@uw.edu>
Cc: Cale Ash <cash@degenkolb.com>, Lee Shipman <lshipman@shoalwaterbay-nsn.gov>, Mitchell Romero <mitchromero@oacsvcs.com>, lkerns@shoalwaterbay-nsn.gov <lkerns@shoalwaterbay-nsn.gov>, Randy J LeVeque <rjl@uw.edu>

Hi Frank,

Thanks for checking in. All the major comments have been adjudicated, except one minor comment raised by Tim Walsh "On Page 3 of the modeling study, in the abstract, please confirm that the units for maximum current speed should be "m/s" not "m."

Would you take a look at the abstract and update the abstract as appropriate? Once this is taken care of, you can go ahead to officially finalize it and archive it. Please let me know if you have any questions.

Thanks

Kent

From: Frank I. Gonzalez <figonzal@uw.edu>
Sent: Tuesday, February 4, 2020 12:33 PM
To: Kent Yu <kentyu@seifconsulting.com>
Cc: Cale Ash <cash@degenkolb.com>; Lee Shipman <lshipman@shoalwaterbay-nsn.gov>; Mitchell Romero <mitchromero@oacsvcs.com>; lkerns@shoalwaterbay-nsn.gov; Randy J LeVeque <rjl@uw.edu>; Frank Gonzalez <figonzal@uw.edu>
Subject: Re: Shoalwater Bay Tsunami Evacuation Tower Peer Review Comment Log

Hi, Kent:

Has our Final Report, "Modeling Study of a Proposed Vertical Evacuation Structure Site for the Shoalwater Bay Tribe" been accepted? If so, we'd like to officially finalize and archive it.

Also, we received notice this morning that a meeting of the Washington Joint Tsunami Workgroup is set for this Thursday, 6 February, so we could report completion of the report to this group, as well.

Thanks,
--Frank

On Thu, Nov 21, 2019 at 5:57 AM Cale Ash <cash@degenkolb.com> wrote:

Kent,

Please find attached the "final-final" versions of the tsunami inundation report (UW author), basis of design (Degenkolb author), and Peer Review Comment Log.

As noted below, we hope this allows us to close out all of the inundation modeling-related comments so we can stay on track to submit for permit in mid-December.

Let us know if a phone call with Ian, Hong-Kie, and others would help facilitate this process.

Thanks,

Cale Ash, P.E., S.E.
Office Director and Principal
Degenkolb Engineers
d: 206.340.8102

Figure A9. Confirmation of acceptance of the final report by representatives of the PAP, PRT, Degenkolb Engineers, and the Shoalwater Bay Indian Tribe